2012-10-03

Measurement of the absolute isotopic composition and atomic weight of molybdenum by multiple collector inductively coupled plasma mass spectrometry

Mayer, Adam John

UNIVERSITY OF CALGARY

Measurement of the absolute isotopic composition and atomic weight of molybdenum by multiple collector inductively coupled plasma mass spectrometry

by

Adam John Mayer

A THESIS
SUBMITTED TO THE FACULTY OF GRADUATE STUDIES
IN PARTIAL FULFILLMENT OF THE REQUIREMENTS FOR THE
DEGREE OF MASTER OF SCIENCE

DEPARTMENT OF PHYSICS AND ASTRONOMY

CALGARY, ALBERTA

SEPTEMBER, 2012

Abstract

Analytical techniques have been developed for measuring the absolute isotopic composition of molybdenum reference materials using multiple collector inductively coupled plasma mass spectrometry. A correction for instrumental mass bias was performed using a molybdenum double-spike prepared from gravimetric mixtures of ^{92}Mo and ^{98}Mo isotope spikes. Careful assessments of laboratory procedures and data were performed to analyze possible impacts on the final results. The absolute isotopic composition of the SCP Science - PlasmaCal molybdenum reference material was determined to be: ^{92}Mo=14.626(17), ^{94}Mo=9.182(5), ^{95}Mo=15.869(5), ^{96}Mo=16.67(3), ^{97}Mo=9.585(3), ^{98}Mo=24.308(14), and ^{100}Mo=9.758(11). The atomic weight of molybdenum in PlasmaCal was calculated as A_{r}=95.9508(16). Delta values (reported as $\delta^{98/85}$Mo relative to PlasmaCal) were determined for: NIST SRM-3134, +0.37(14)‰; Johnson-Matthey pure molybdenum rod, -0.32(14)‰; BCR-2, +0.28(14)‰; and SDO-1, +1.5(5)‰. The total natural variation of molybdenum of -1.5‰ to +3‰ results in a calculated atomic weight of A_{r}=[95.948, 95.956].

Acknowledgements

I would like to thank Dr. Michael Wieser for his guidance throughout the entire project. I would also like to thank Dr. Robert Loss for his meaningful discussions on the double-spike technique and his work getting this project started. I would like to thank Bernadette, Hali, Monika, Nenita and Jesusa for their help with the chemistry and sample preparation. Finally, I would especially like to thank my family and friends for their support and encouragement over the years.

Table of Contents

List of Tables

List of Figures and Illustrations

List of Symbols, Abbreviations and Nomenclature

Symbol	Definition
MC-ICP-MS	Multiple-collector inductively-coupled-plasma mass spectrometer
TIMS	Thermal ionization mass spectrometer
SEM	Secondary electron multiplier
IUPAC	International Union of Pure and Applied Chemistry
NIST	National Institute of Standards and Technology
USGS	United States Geological Survey
ORNL	Oak Ridge National Laboratory
^{96}Mo	Isotope of molybdenum with mass number 96
‰ (permille)	parts per thousand
95.96(2)	95.96±0.02, absolute uncertainty at 1 s.d.
Ga	Billions of years before present
Isotope spike	Material that has been highly enriched in one or more isotopes of an element
Isotopic fractionation	A relative change in the isotopic composition of an element due to some process

Chapter 1

Introduction

Molybdenum is a chemical element with an atomic number of 42. It has seven isotopes with mass numbers of 92, 94, 95, 96, 97, 98 and 100. Among the elements, the isotopic composition of molybdenum is unique, since all seven isotopes have fairly similar relative abundances, as shown in Figure 1.1.

Molybdenum is most commonly used in the manufacture of steel alloys[18] as it readily forms hard, stable carbides and has the sixth highest melting point of naturally occurring elements. It is also used in various compounds such as molybdenum disulfide, which is a solid lubricant[19]; molybdenum disilicide, which is an electrically conducting ceramic; and molybdenum trioxide, which is an adhesive to bond enamels and metals. Molybdenum also plays an important role in biochemistry, for example certain enzymes involved with nitrogen fixation contain molybdenum[20].

The isotopic composition of molybdenum from different natural samples has become more of interest over the last decade as research groups are finding new applications such as studies of the molybdenum isotopic composition in ocean sediments[21, 22, 23], zircons[24], meteorites[25], and natural fission reactors[26] which are discussed in Chapter 2. With many laboratories publishing data on variations in the isotopic composition of molybdenum, it has been difficult to compare the results between laboratories as there is no established standard reference material for the isotopic composition. Each group compares their results to an internal laboratory standard that can have a different isotopic composition to one from a different laboratory. The variations in the isotopic composition of molybdenum that are reported are no more than 5 ‰ (parts per thousand) and significant effects result in variations less than 1 ‰. The variation of the isotopic composition of the different laboratory standards

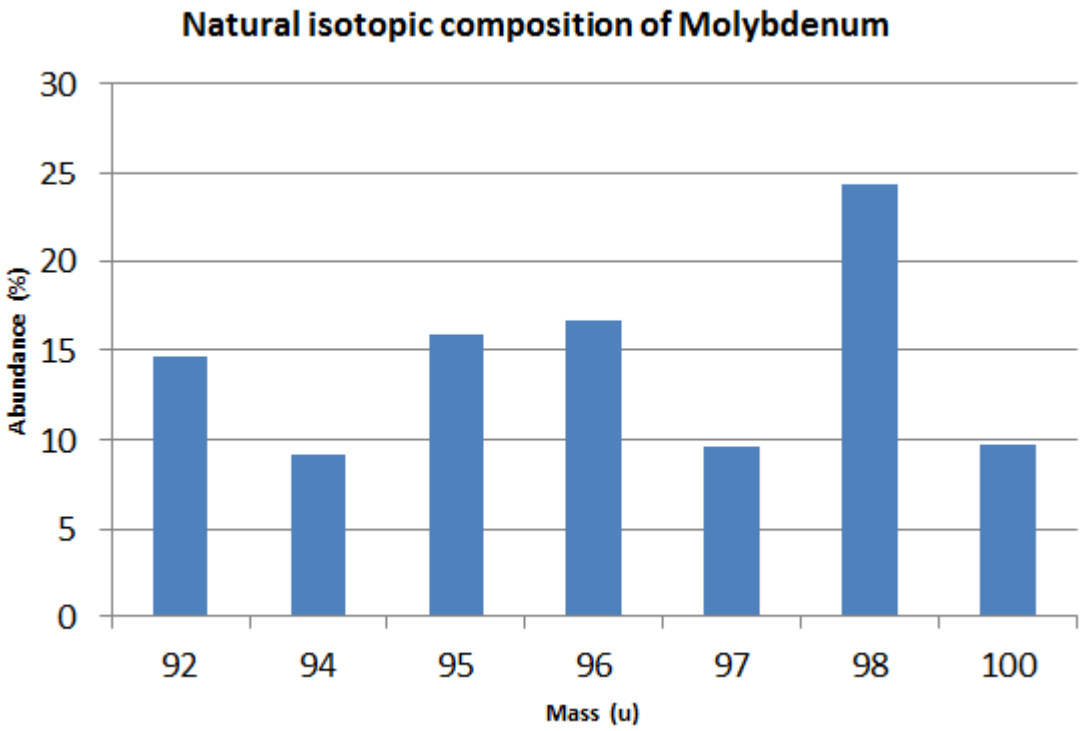

Figure 1.1: Natural isotopic composition of molybdenum.

can be as much as 1-3 ‰, making it impossible to compare results between laboratories. It is becoming increasingly important to establish a common reference material with a known isotopic composition that is readily available to all laboratories in the world. I aim to develop a method for measuring the absolute isotopic composition of molybdenum, free from any measurement biases, and apply this method to establish the absolute isotopic composition of various internationally available molybdenum reference materials. These reference materials have not yet been calibrated for isotopic composition, and only have known molybdenum concentrations.

The atomic weight of molybdenum in a sample is determined directly from the absolute isotopic composition. The current published value for the atomic weight of molybdenum by IUPAC is A_{r}=95.96(2)[27] and has an uncertainty which can be improved substantially with modern measurement techniques using the Thermo Scientific Neptune mass spectrometer. In this thesis, I will explain the technique used to produce a fully calibrated measurement

of the atomic weight of molybdenum, with the eventual plan of submitting the new value to the IUPAC Commission on Isotopic Abundances and Atomic Weights (CIAAW).

In the next chapter, I will discuss the necessary background for the topic of this thesis. I will review the history of atomic weight determinations and mass spectrometry and follow with an overview the instruments and measurement techniques currently being used today for mass spectrometry, with a discussion of the Neptune mass spectrometer. I will finish with a brief review of recent work on the measurement of the isotopic composition and atomic weight of molybdenum.

In Chapter 3, I will define isotopic fractionation and describe how and when it occurs. I will describe the models and mathematical laws used to describe it, and explain how these models can be used with the double-spike technique to quantify and correct for the isotopic fractionation introduced in the laboratory. Finally, I will explain how to monitor and rectify changes of the instrumental mass bias between measurements and from day to day.

In Chapter 4, I will discuss laboratory procedures for preparing and calibrating the molybdenum double-spikes. I detail the procedures used to weigh and mix the pure metal molybdenum spike materials. This is followed by an overview of the operation of the Neptune MC-ICP-MS. Finally, I will describe the results and analysis used to calibrate the molybdenum double-spike.

In Chapter 5, I will discuss the measurement and calculation of the absolute isotopic composition of various synthetic and natural reference materials. I begin with a discussion of pure molybdenum samples and the calculation of their absolute isotopic compositions. Then I will discuss the application of the double-spike method to measuring natural reference materials obtained from the USGS including an overview of the chemistry required to prepare the samples for analysis.

Chapter 6 is dedicated to discussing the various challenges that were encountered throughout the thesis project, and the experiments that were performed to solve the problems. These

have been set aside so as to not interrupt the flow of the preceding chapters. I will begin by discussing the problem of electro-static charge build up on the Teflon containers used during double-spike preparation. I will then discuss a set of tests performed to find a solution to the static charge problem. Finally, I will discuss drift in the $^{92}Mo/^{95}Mo$ isotope abundance ratio of the PlasmaCal molybdenum standard that was discovered when compiling all of the data.

In the final chapter, the results of the thesis project are summarized, and the outcomes and accomplishments are explained.

1.1 Objectives of thesis research project

1. To develop an algorithm for fully calibrating the molybdenum double-spike.

2. To apply the double-spike to measuring the absolute isotopic composition of various molybdenum reference materials and to establish a molybdenum reference material suitable for inter-laboratory comparison.

3. To calculate the atomic weight of molybdenum with increased precision over the current IUPAC published value, and submit the value for consideration for the periodic table of the elements.

Chapter 2

History and Background

2.1 Introduction

In this chapter, I will be discussing the history of atomic weight determinations and mass spectrometry followed by an overview of recent work on the measurement of the isotopic composition and atomic weight of molybdenum. I will then review the instruments and measurement techniques currently being used today for mass spectrometry, with a discussion of the Neptune multiple collector inductively coupled plasma mass spectrometer (MC-ICP-MS).

2.2 History of atomic weight determinations

The 1914 Nobel Prize in Chemistry was awarded to Theodore W. Richards for his pioneering work in accurately measuring the atomic weight of a large number of elements[28]. At this time, the technique developed was called the Harvard Method. The method used accurate gravimetric measurements using chemical stoichiometry and was able to produce accurate results that were used until the 1970s[29].

Contemporary with Richards' work in chemistry was J.J. Thomson's research in mass spectrometry. In 1912, he discovered that neon existed in two isotopic forms of mass 20 and 22. This explained why neon had an atomic weight of 20.2, which was expected to be a whole number. Approximately 10 % of neon exists with mass 22, while 90 % exists with mass 20, resulting in an average mass of 20.2. Using a chemical method to determine the atomic weight of an element will give the weighted average mass of the element.

Thomson's research was continued by his colleague and graduate student Francis W.

Aston. Aston developed more sensitive mass spectrographs which he used to discover the isotopes of a large number of stable elements. He was awarded the 1922 Nobel Prize in Chemistry for this work. By 1942, Aston had determined the isotopic compositions of most of the elements.

Similar research was being done by other physicists including Arthur Dempster, who developed the first modern mass spectrometer, and Alfred Nier. In the early 1920s, Dempster determined the atomic weights of several elements by measuring the relative isotope abundances and assuming each isotope had a whole numbered mass. This is the method that is still used today, except the mass of each isotope is now known to very high precision. This physical method of measuring atomic weight became the standard, replacing the Harvard or chemical method in the late 1970s. The chemical method was unable to produce results for the atomic weight of gallium that were within agreement of the physical method. At the same time, the physical method was able to produce increasingly precise results that were orders of magnitude more precise than the chemical method.

Throughout history, the atomic weights of the elements had been regarded as constants of nature. This was first challenged with the discovery of radioactivity, where individual isotopes decay thus changing the atomic weight of the material over time. The amount of the decaying isotope will decrease, while the amount of the daughter isotopes will increase. At first it was hypothesized that only elements involved with radioactive decays would have varying atomic weights. It was then discovered, in 1939 by Nier and Gulbransen, that the relative abundance of ^{13}C varies by as much as 5 % in nature. As analytical techniques improved for different elements, it was seen that relative isotope abundances varied for all of the light elements, and that the variations could be caused by natural processes. This is referred to as natural isotopic fractionation, and can be caused by a large variety of processes including biological, geological, chemical, physical and nuclear processes.

Changes in isotopic composition due to natural processes can be quite small, much less

than 1 ‰ per mass unit for many elements. Therefore the development of more and more advanced mass spectrometers was required to detect the variations. More recently, modern mass spectrometers have been used to measure variations in what are called "non-traditional elements", such as iron, molybdenum, and cadmium. These results have been used to further understand natural processes, and to gain insight into processes that occurred thousands or even billions of years ago. For example, measurements of nickel and magnesium isotope abundances in meteorites have been used to set constraints on models of the formation of the solar system. Different applications will be discussed further at the end of this chapter

The atomic weight of an element depends directly on the isotopic composition of that element. Since the isotopic composition varies in nature, the same is true of the atomic weight. Modern measurements of the atomic weight of an element take into account the best possible measurement of the atomic weight of a sample, as well as the natural variation in nature. This has led to a change in the way atomic weights are reported for some of the lighter elements. Rather than publishing an average value with some uncertainty, the atomic weight is reported as a range of values that occur in nature. For many elements, the atomic weight of a sample can be determined very precisely, but the natural variation is far greater.

2.3 Molybdenum isotopic composition measurements

2.3.1 Historical atomic weight and isotopic composition measurements

In the early 1900s, the atomic weight of molybdenum was measured to be a whole number. This led to the initial belief that molybdenum had only a single isotope at mass 96. In 1931, Aston produced the mass spectrum of molybdenum using his mass spectrograph and detected seven isotopes at masses 92, 94, 95, 96, 97, 98 and 100[30]. Using photometry with his mass spectrograph, he was able to measure the relative abundance of each isotope to within $\sim$1 % of modern measurements. This isotopic composition was used to determine an atomic weight for molybdenum of 95.97 $\pm$ 0.06, which was in agreement to the chemically

determined value.

The current IUPAC value for the atomic weight of molybdenum was measured by Wieser and De Laeter in 2007[1]. This was the first calibrated measurement with synthetic isotope mixtures using thermal ionization mass spectrometry. The atomic weight published by IUPAC is 95.96(2)[27] which was higher, though within uncertainty of the previous value of 95.94(2). The previous value, which remained relatively unchanged since 1938 was based on chemical measurements, as well as uncalibrated isotopic composition measurements. Further work is necessary to confirm the higher atomic weight value and to increase the precision substantially using MC-ICP-MS.

2.3.2 Application to paleoceanography

Mass dependent variations in the isotopic composition of molybdenum were only discovered in 2001. J. Barling et al. reported natural isotopic fractionation in ocean sediments deposited under anoxic conditions as well as molybdenum in ferromanganese nodules[21]. Siebert et al. performed similar measurements on seawater and crustal samples also finding natural isotopic fractionation[22]. Siebert suggested that the narrow range of compositions for crustal Mo sources indicate that isotopic fractionation by chemical weathering and magmatic processes is insignificant on a global scale. However, isotopic fractionation in seawater samples suggest that fractionation can occur under oxic conditions. The isotopic composition of the molybdenum in seawater will therefore be dependent on the oxic and anoxic conditions. The range of variation in the isotopic composition of molybdenum in natural samples is outlined in Figure 2.1.

A recent article by Lyons[31] describes the importance of the molybdenum isotope system as a tracer of changes in ocean redox on a global scale. The article summarizes recent studies of past redox conditions in the oceans, and finishes by discussing some of the concerns in using the molybdenum isotope system as a ocean redox tracer such as the isotope systematics of conversion between MoO_4^{2-} and MoS_4^{2-}.

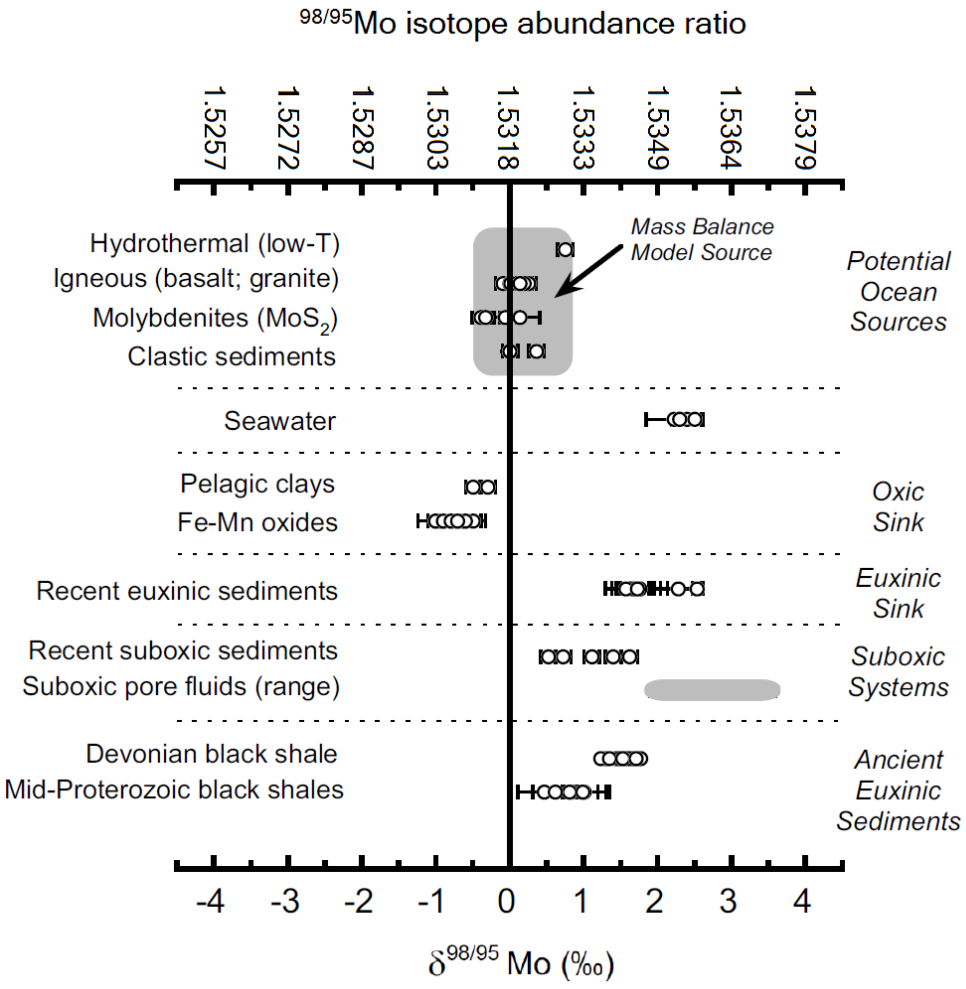

Figure 2.1: Natural variation of molybdenum isotopic composition, modified after Anbar[7]. $\delta^{98/95}$Mo represents the relative change of the isotope ratio in permille.

More recently, the isotopic composition of molybdenum has been used in models to constrain the levels of free oxygen in the atmosphere. Czaja et al. discuss measurements of the isotopic compositions of iron and molybdenum in carbonates and shales from ∼2.68 to 2.50 billion years ago (Ga)[23]. Based on the coupled iron and molybdenum isotopic composition data, they suggest that oxygenic photosynthesis in the ancient shallow ocean was required to have evolved by at least 2.7 Ga, prior to the Great Oxidation Event of ∼2.2-2.4 Ga, meaning that the Neoarchean ocean may have had a different oxygenation history than that of the atmosphere.

2.3.3 Application to cosmochemistry

Molybdenum isotope anomalies in certain meteorite samples were observed by Dauphas et al. in 2002[25]. The anomalies suggested an excess in p- and r-process nuclides and a mirror deficit in s-process nuclides. Isotope heterogeneity of various elements in meteorites has been used to support and place constraints on models for the formation and evolution of the early solar system. Also, the abundances of important isotopes such as p-process nuclides are important in developing models for nucleosynthesis. Isotope abundance measurements of this type must be fully calibrated in order to be applicable.

2.3.4 Application to nuclear physics

In 2001, Wieser and De Laeter published results of their measurements of molybdenum extracted from geologically old zircons[24]. Enhanced levels of ^{96}Mo were suggested to have been caused by double β decay of ^{96}Zr. The experimental data indicated that the half-life of ^{96}Zr double β decay is (9.4±3.2)*10^{18} yr, which agreed with the theoretically predicted half-life.

In a recent article published by Wieser and DeLaeter, the isotopic composition of molybdenum in six uranium-rich samples from the natural reactor site in Oklo, Gabon were measured[26]. The site behaved as a natural nuclear fission reactor in Precambrian times.

Molybdenum is useful to analyze as it has three isotopes (^{92,94,96}Mo) which are unaffected by the fission process, while the remaining isotopes are. This enabled relative fission yields of molybdenum to be calculated from the isotopic composition measurements. The results were used to demonstrate that the most important nuclear process involved in the Zone 9 reactor was the thermal neutron fission of ^{235}U.

2.3.5 Search for a molybdenum isotopic reference material

The need to establish a common standard reference material for molybdenum have prompted some research groups to publish measurements of available molybdenum reference materials. Greber et al. recently published measurements of the $\delta^{98/95}$Mo values and molybdenum concentration data for three NIST standard reference materials including NIST SRM 610, 612 and 3134[32]. They suggest that NIST SRM-3134 is a highly suitable isotopic reference material for molybdenum. Similar work was published by Wen et al. in 2010, also suggesting NIST SRM-3134 as the "delta-zero" standard reference material[33].

Although there have been several measurements of the relative isotopic composition of molybdenum in different reference materials, there has not yet been a measurement of the absolute isotopic composition of molybdenum of a standard reference material. It remains important to measure the absolute isotopic composition of a readily available reference material, to establish an isotopic standard reference material suitable for inter-laboratory comparison of molybdenum isotope data.

2.4 Mass spectrometry

Modern mass spectrometers have evolved from the original designs by J.J. Thompson and other contemporaries. Mass spectrometers consist of three basic sections: the ion source, the mass analyzer, and the detector. The design of these components can vary substantially depending on the type of mass spectrometer and the application, but the basic concept of

each remains the same. The ion source generates the necessary ions, the mass analyzer separates the ions depending on their mass, and the detector measures the amount of the selected ions.

2.4.1 Ion source

There are many different types of ion sources. The most commonly used sources in isotope ratio mass spectrometry include the gas source, the solid source (thermal ionization), inductively-coupled-plasma (ICP), and secondary ion.

Measurements of lighter elements are typically performed using a gas source mass spectrometer, where a sample is introduced as a pure gas and ionized, usually by electrons emitted from a hot filament. This is used in gas chromatography mass spectrometry (GC-MS), which is the most common type of mass spectrometer and is used in fields including forensics, environmental monitoring, food and drug analysis and medicine.

In thermal ionization mass spectrometry (TIMS), a liquid sample is deposited onto a filament and evaporated, leaving a solid residue. The filament is loaded into the mass spectrometer and heated to ionize the residue. TIMS is used to measure the isotope abundances of many different elements, and was the most popular technique before the advancement of ICP-MS.

The ICP ion source consists of a plasma which ionizes an introduced sample. The sample is usually introduced as a fine mist using a nebulizer. This converts a liquid sample into an aerosol that enters the plasma and is ionized. ICP-MS has a wide variety of applications and is becoming more popular in isotope abundance measurements, as it is more effective at ionizing some elements.

The secondary ion source uses an ion gun which bombards a target with ions, releasing secondary ions from the target. This source is commonly used in materials science, and can directly analyze solid surfaces and thin films.

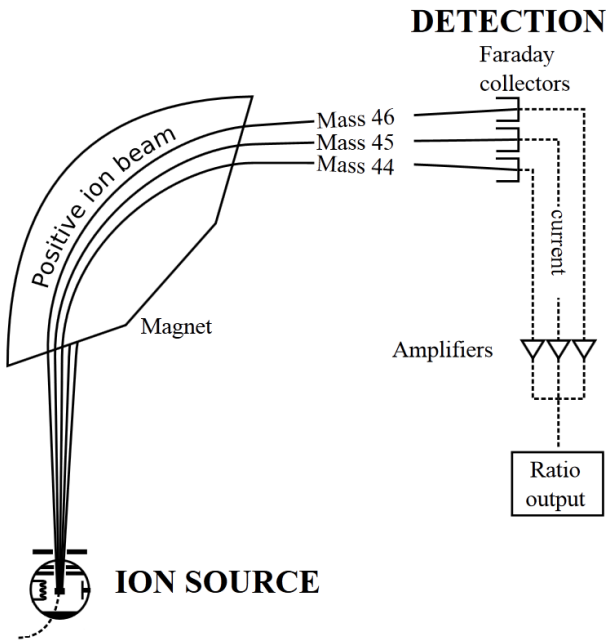

Figure 2.2: Diagram of a basic magnetic sector.[8] The ions formed in the source are separated according to their mass in the magnetic field, then collected in the Faraday cup detectors.

2.4.2 Mass analyzer

The purpose of the mass analyzer is to separate the ions according to their mass. The most common designs for use in isotope analysis are called sector instruments. These consists of magnetic and/or electric fields, which are used to focus and separate the ions. This type of mass analyzer is used for this project, and will be discussed in more detail later in this chapter. They are suitable to isotope analysis because of their high mass resolution. This allows the analyzer to completely separate neighboring isotopes, and when necessary to separate compounds that nearly overlap an isotope, such as $^{40}Ar^{16}O^{+}$ and $^{56}Fe^{+}$. Also, modern magnetic sector mass spectrometers have multiple detectors, which allow for the simultaneous collection of nearby isotopes, for example all isotopes of iron and nickel. This is important for isotope abundance ratio measurements as the intensities of the measured ion currents can vary over short periods of time, but the variation affects all isotopes simultaneously such that the ratio of the ion current of one isotope to another remains fairly constant. A diagram of a basic magnetic sector is in Figure 2.2

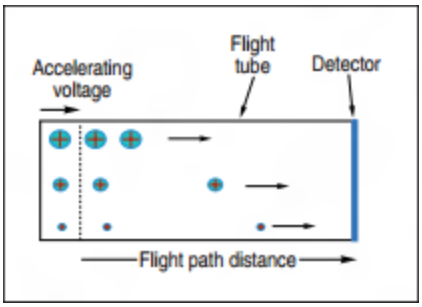

Figure 2.3: Diagram of a Time-of-flight analyzer.[9] The ions have equal kinetic energy so their speed is dependent on their mass. The time to travel the same distance will depend on the mass.

Time-of-flight analyzers use the simple equation $E_k = \frac{1}{2}mv^2$ to separate ions of different mass. All uniformly charged ions are given the same kinetic energy by accelerating them through the same electric potential. They then travel over a uniform distance, and are detected at different times, dependent on their mass as shown in Figure 2.3. The advantage of the time-of-flight analyzer is that it is able to measure ions with different masses together, even if the mass difference is large. However, they do not offer the same mass resolution as magnetic sector instruments.

A quadrupole mass analyzer filters ions by generating an electric field between four parallel rods. A DC voltage is applied to one pair of rods opposite each other, while a RF voltage is applied to the other pair of rods. This allows ions of only a specific mass to charge ratio to reach the detector, as shown in Figure 2.4. The quadrupole mass analyzer was the first mass analyzer to be developed for ICP-MS in the 1980s, and is used in most commercial applications. The advantage of the quadrupole mass analyzer is its high scanning speed and short analysis time. It is not suitable for this project since it has a lower mass resolution more suitable to element analysis, and cannot measure different isotopes simultaneously resulting in low precision for isotope abundance ratio measurements.

Ion traps use a combination of electric and magnetic fields to capture ions with a specific charge and mass. These can be used to make very high precision isotopic mass measurements. For example, TITAN at TRIUMF has been used to measure the mass of exotic, short-lived

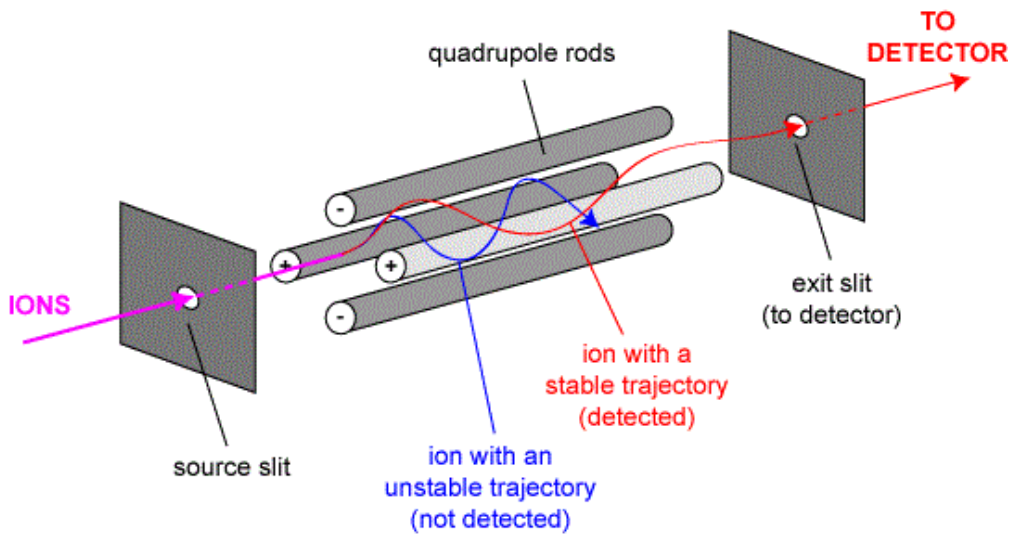

Figure 2.4: Diagram of a quadrupole mass analyzer.[10] Only the ions with the correct mass to charge ratio arrive at the detector, while the others have an unstable path and exit the quadrupole.

nuclides such as ^{8}He, and to make ppb measurements of the mass of stable isotopes. A basic diagram of a Penning ion trap is shown in Figure 2.5

2.4.3 Detector

The final stage of a mass spectrometer is the detector. In isotope ratio mass spectrometry, after the ions have been separated according to their mass, they are collected and the number of ions is measured. For most applications, a Faraday cup is used to capture the ions and

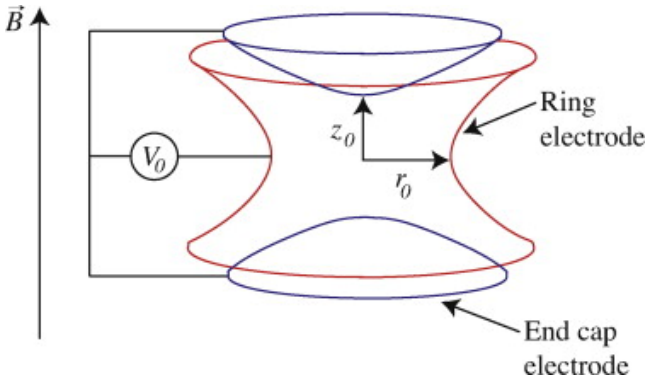

Figure 2.5: Diagram of a Penning ion trap.[11] The ions with the correct mass to charge ratio are trapped inside the electromagnetic fields.

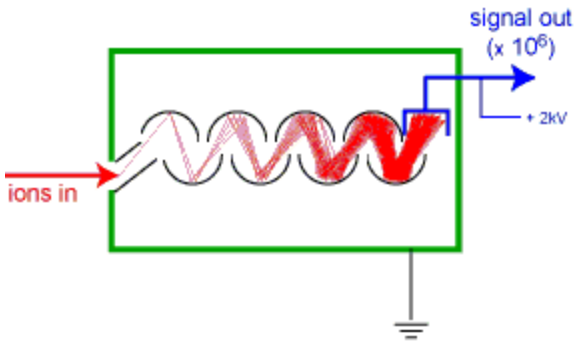

Figure 2.6: Diagram of a secondary electron multiplier.[12] Individual ions can be detected by multiplying the signal they generate many times.

generate a current which can be measured as a voltage across a high ohmage resistor (often 10^{11} Ω). For example, a 10^{-11} A ion current measured across a 10^{11} Ω resistor will be measured as 1 V. When a smaller number of ions are being detected, less than 100 000 per second, a more sensitive detector is necessary. This is usually a secondary electron multiplier, which consists of a chain of dynodes. When an ion enters the detector, it strikes the first dynode which releases a packet of electrons. These in turn are accelerated into the next dynode which releases a larger number of electrons. This continues until a large enough packet of electrons is generated to measure, as shown in Figure 2.6. The secondary electron multiplier is effective over a range of individual counts up to a couple hundred thousand, at which point the large number of ions will damage the detector. Modern isotope ratio mass spectrometers will consist of several Faraday cups which are positioned to simultaneously measure several masses, and an SEM or other ion counter to measure low abundance isotopes.

2.4.4 MC-ICP-MS for molybdenum isotope analysis

The measurement of the isotopic composition of molybdenum is typically performed using a multiple collector ICP-MS (MC-ICP-MS). Although TIMS has been used in the past, it can be difficult to ionize molybdenum using a filament, and requires complicating sample deposition procedures that are not always successful. It requires relatively large amounts of molybdenum, around 1 μg, to produce small ion currents (0.1 V per isotope). MC-ICP-MS

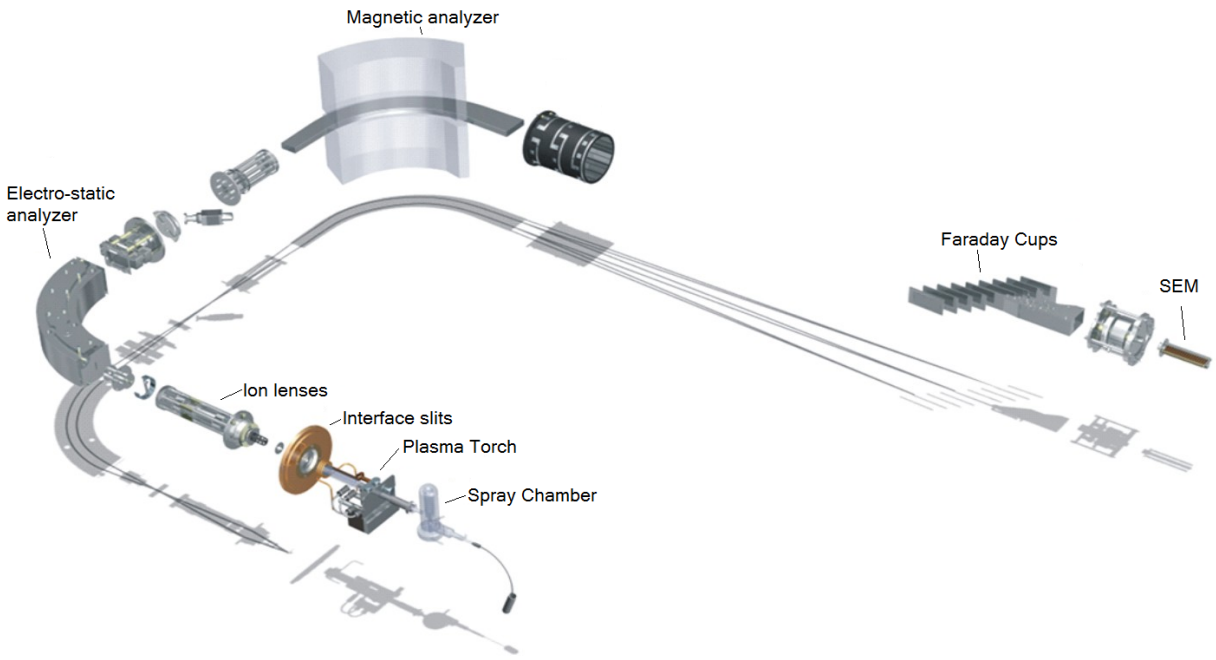

Figure 2.7: Diagram of the Neptune MC-ICP-MS used at the University of Calgary isotope science laboratory.[13]

has proven to be both highly reliable and highly sensitive for measurements of molybdenum. Only 200 ng are necessary to generate an ion current of 2-3 V per isotope. At the University of Calgary stable isotope lab, we use a Thermo Scientific Neptune MC-ICP-MS set up to simultaneously measure the seven isotopes of molybdenum on 10^{11} Ω resistors, while ^{91}Zr is monitored on a 10^{12} Ω resistor. It was not possible to collect the major isotope of zirconium ^{90}Zr, and ^{100}Mo at the same time due to the large mass difference. A diagram of the Neptune MC-ICP-MS is shown in Figure 2.7, and the process is described below.

Molybdenum samples are dissolved in 3 % HNO_3, which is naturally aspirated through a nebulizer into a cyclonic spray chamber, shown in Figure 2.8. Larger droplets, which are more difficult to ionize, are drained from the spray chamber, while smaller droplets pass into the plasma torch.

Argon flows through the torch which is made up of concentric quartz tubes[34]. The top of the torch is surrounded by a load coil, which is powered by a 1200 W radio-frequency generator. A spark releases free electrons from argon atoms, which, in the intense electro-

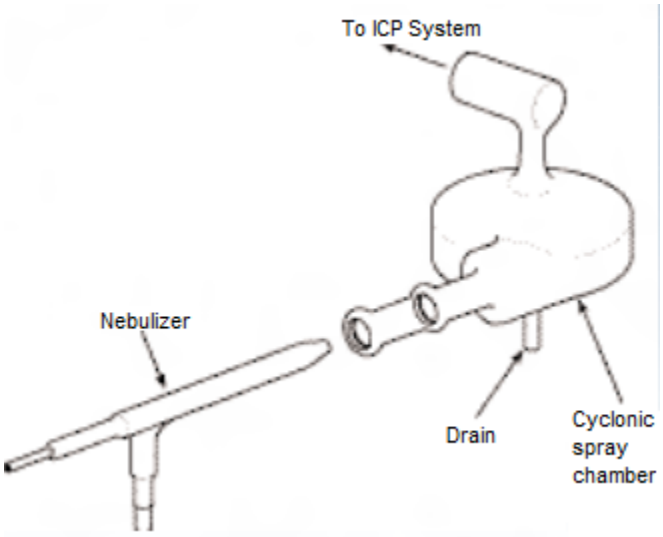

Figure 2.8: Diagram of a glass nebulizer and cyclonic spray chamber.[14]

magnetic field generated by the load coil, collide and ionize other argon atoms in a chain reaction resulting in an inductively coupled plasma. The plasma has a temperature range of 6000-10 000 K. It is possible for the plasma to form an electrical discharge and arc to the interface region. This has negative effects including increasing the kinetic energy spread of the ions, and damaging the interface. To keep this from happening, the Neptune capacitively decouples the plasma from the load coil by using a grounded guard electrode.

The droplets coming from the spray chamber enter the plasma torch, where they are desolvated, vaporized, atomized and then ionized. The ions then pass into the interface region, where the pressure drops from atmospheric pressure down to the vacuum of the analyzer. The interface region consists of two metallic cones, usually made of nickel. The first cone, called the sampler cone, has a small orifice with a diameter of around 0.8-1.2 mm. The second cone, called the skimmer cone, is sharper and has a smaller orifice with a diameter of around 0.4-0.8 mm. The housing is made of copper and water cooled since it is adjacent to the hot plasma. The interface region is held at $\sim$2 Torr by a mechanical roughing pump. The plasma torch and interface region are shown in Figure 2.9

After the ions have passed through interface region, they enter the ion optics. The ion

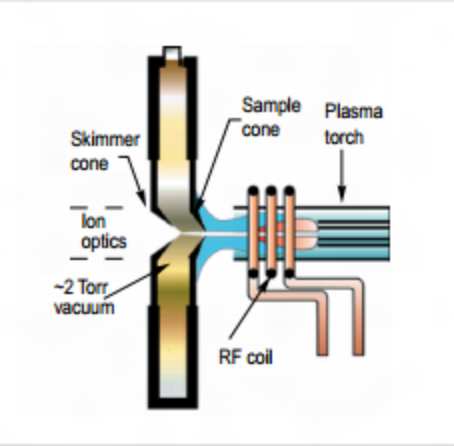

Figure 2.9: Diagram of the plasma torch and interface region.[15]

optics are made up of a series of electrostatic lenses which serve to focus and accelerate the ion beam, and separate the positive ions of interest from the remaining particulates, negative ions, electrons, photons and neutral particles. Any of the latter that enter the analyzer region will increase the background levels at the detectors. The first component of the lens system is the aperture, which, in the Neptune, is made of graphite to reduce sputtering caused by the bombardment of a large number of ions. This further reduces energy spread and measurement noise. After this, the extraction lens, which is held at a constant potential of -2000 V is used to accelerate and focus the ions, while other lenses are used to further focus and aim the ions. The ion optics are held at $\sim 10^{-3}$ Torr by a turbo-molecular pump.

The focused ion beam then enters the first sector of the mass analyzer, which is held at $\sim 10^{-7}$ Torr by a large turbo-molecular pump. The first component is the electric sector, consisting of an electric field which deflects the path of the ions by 90°. The electric sector is dispersive with respect to ion kinetic energy, and so filters the kinetic energy of the ions, narrowing the range of kinetic energy that makes it through the electric sector. The filtered ions then pass into the magnetic sector, which deflects the path of the ions by another 90°. This relies on the Lorentz force, $\vec{F} = q\vec{v} \times \vec{B}$, which causes ions of different mass to charge ratio to have a different radius of curvature. The ions of interest will exit the magnetic field, while the remainder will not leave the flight tube. The magnetic field and detector sections

are held at $\sim 10^{-9}$ Torr by an ion pump.

The ions, which have been separated according to their mass, are then collected in multiple Faraday cups, or a secondary electron multiplier when necessary. The ions striking the Faraday cups generate an ion current which is measured as a voltage across a 10^{11} Ω resistor, or 10^{10} Ω or 10^{12} Ω resistors if necessary. All seven molybdenum isotopes are collected on Faraday cups simultaneously, along with ^{91}Zr to monitor the potential zirconium interferences at masses 92, 94 and 96. These isotopes of zirconium have very nearly the same mass as the respective molybdenum isotopes of the same mass number (m(^{92}Zr) = 91.9050), m(^{92}Mo) = 91.9068), and so their signals are indistinguishable. By monitoring the intensity of ^{91}Zr, a correction was applied to the molybdenum isotopes with zirconium interferences based on the standard isotopic composition of zirconium. This correction can produce uncertainty in the molybdenum isotope ratios, so if the interference was too large (>5 mV at ^{91}Zr), the sample results were not used.

The gain factor of the amplifier describes the recorded voltage compared to the ion current at the Faraday cup. Each amplifier has slightly different gain factors which can change over time. In order to ensure that the measured isotope ratios are not affected by amplifier gain differences, automated gain calibration was performed at least once per week. This consists of a known current being applied to each amplifier, and recording the measured output. This allows for a gain correction factor to be applied, ensuring accurate measurements are recorded.

After letting the instrument reach stable operating conditions for at least an hour the instrument parameters were optimized. While monitoring the ion currents on the Faraday cups, the plasma conditions including the sample and auxiliary gas flow rates and torch positions were adjusted for best signal intensity and stability. Then the focus settings were fine tuned to give the best signal having both high intensity and a good peak shape with a flat top and sharp edges. The peak shape is measured by deflecting the ion beam outside

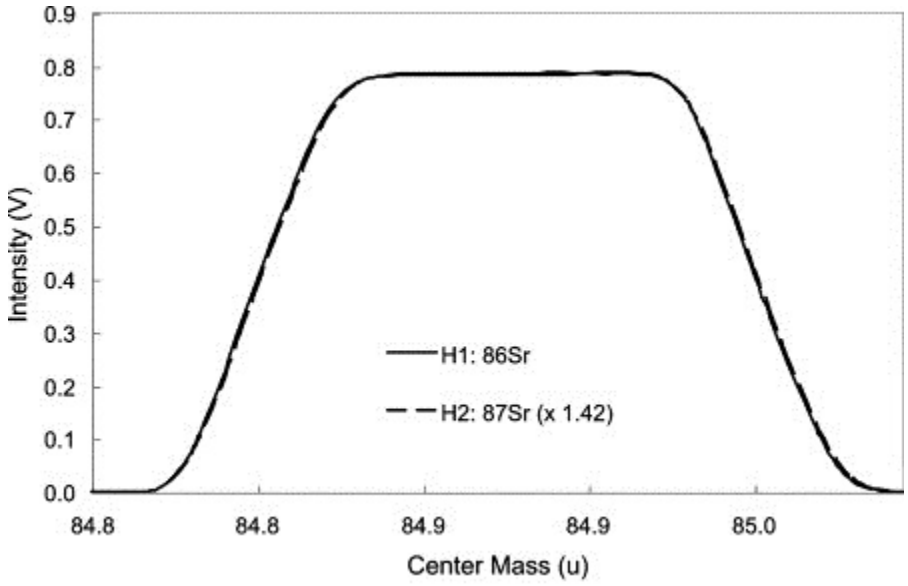

Figure 2.10: Example of a peak scan for ^{86}Sr and ^{87}Sr[16]. The flat top is important so that slight changes in the deflection in the ion beam do not change the measured intensity. The overlapping peaks are necessary to ensure that the ion beam for each isotope is aimed at the centre of each Faraday cup.

the Faraday cup on one side then sweeping across the Faraday cup all the way until it is clear on the other side. An example of good peak shape is in Figure 2.10. Before each sample measurement, peak centering and baseline measurement are performed. The peak centering ensures that the center of the ion beam is exactly at the center of the Faraday cup. The baseline procedure measures the electronic baseline by defocussing the ion beam so no ion beam is incident on the Faraday cups, and recording the electronic noise for 30 s. The measurement software then collects the data for all measured isotopes simultaneously. When collecting data, the voltage is measured at each Faraday cup for 8.134 seconds per cycle. The average of each voltage measurement for each isotope is divided by the voltage measurement for the reference isotope to determine the isotope ratios (e.g. ^{98}Mo signal intensity divided by ^{95}Mo signal intensity for 98/95 Mo isotope ratio). While the intensity of each ion beam varies over a measurement cycle, the ratio of one ion beam to another is more constant in time. Typically a set of around one hundred cycles are measured.

2.5 Conclusion

The study of atomic weights has evolved substantially over the past century. Thomson's first spectrograph showed that elements can have distinct isotopes, confirming that atomic weights are not whole numbers. Though the initial measurements were performed using stoichiometry, the pioneering work of Aston to develop more powerful mass spectrographs to determine the isotopic composition of most of the elements led to the modern technique for determining atomic weight. With many different instruments available, it is important to choose the instrument most suited to the measurement required. The atomic weight of molybdenum can be best measured by MC-ICP-MS, since the ion source is most capable of producing molybdenum ions. The precision and accuracy of the atomic weight of molybdenum can be greatly improved using MC-ICP-MS.

Chapter 3

Isotopic Fractionation

3.1 Introduction

In this chapter, I will define isotopic fractionation and describe how and when it occurs. I will describe the models and mathematical laws used to describe it, and explain how these models can be used with the double-spike technique to quantify and correct for the isotopic fractionation introduced in the laboratory. Finally, I will explain how to monitor and rectify changes in the instrumental mass bias between measurements. At the end of this chapter, I include a flow chart to visualize the process in Figure 3.3.

3.2 Definition

Isotopic fractionation is a change in the isotopic composition of an element as the result of different processes. For example, during of the evaporation of water, lighter molecules of H_2O transition from liquid to gas at a higher rate than heavier molecules. This will result in relatively more of the lighter molecules, such as $^{1}H_2{}^{16}O$, in the gas phase, while there are relatively more of the heavier molecules such as $^{2}H_2{}^{18}O$ molecules in the liquid phase. The substance has a relatively lighter isotopic composition after the process (evaporation) compared to before. Isotopic fractionation can also occur in the laboratory during sample preparation and analysis. There are two general types of isotopic fractionation: mass dependent and mass independent. Mass dependent fractionation occurs in processes which favor either heavier or lighter isotopes, and will change the isotope composition accordingly. The evaporation described above is an example of mass dependent fractionation. Mass independent fractionation is a change the isotopic composition that does not depend on mass. For

example, during nuclear decay the abundance of a single isotope of an element could become depleted, while the abundances of the remaining isotopes of the same element remain constant.

The process of measuring the isotopic composition of a sample can introduce further isotopic fractionation, known as mass bias, which will interfere with detecting natural fractionation. It can occur during chemical processing to purify the sample, or in the mass spectrometer itself. The main cause of isotopic fractionation in the mass spectrometer is suspected to be at the interface region[35], where the large number of ions colliding with the slits can develop a space charge thus deflecting the path of the ions. The lighter ions are deflected more, resulting in relatively more heavier ions entering the mass spectrometer.

In most applications, we are only interested in the relative changes in isotopic composition as opposed to the isotopic composition of a specific sample. Changes in the isotopic composition from one sample to another are informative of the processes that occurred to change the composition. Measuring the relative change of the isotopic composition is more straight forward than measuring the actual isotopic composition, since instrumental mass bias does not need to be corrected for. If the fractionation from the measurement process is constant, it will be canceled out while comparing the results for different samples, which will be explained later in this chapter. However, for the determination of the absolute isotopic composition, which is the true isotopic composition without any instrumental mass bias, the fractionation caused by the measurement process must be quantified and corrected in order to produce accurate results. The absolute isotopic composition is important to establish a standard reference material for molybdenum with a calibrated isotopic composition, and is necessary to accurately measure the atomic weight of molybdenum.

3.3 Mass Fractionation Laws

Fractionation laws are used to model mass dependent fractionation by relating the isotope ratios before a process has occurred to the isotope ratios after a process has occurred. In the case of instrumental mass bias, the fractionation law will compare the measured isotopic composition with the true isotopic composition. Isotopic composition measurements are taken as the ratio of the abundance of one isotope to another. The isotopic composition of a sample will be given as a set of isotope ratios, with the abundance of each isotope being compared to one reference isotope. For example, the isotopic composition of molybdenum, which has isotopes of mass 92, 94, 95, 96, 97, 98, and 100, would be reported as the isotope ratios: ^{92}Mo/^{95}Mo, ^{94}Mo/^{95}Mo, ^{96}Mo/^{95}Mo, ^{97}Mo/^{95}Mo, ^{98}Mo/^{95}Mo, and ^{100}Mo/^{95}Mo. Mass fractionation laws follow this general form:

$$R_i = R_{0,i} * F(m_i, m_{\text{ref}}) \tag{3.1}$$

where R_i is the isotope abundance ratio of the ith isotope to the reference isotope after the process; $R_{0,i}$ is the ratio before the process; and $F(m_i, m_{\text{ref}})$ gives the magnitude of the change in the isotope ratio. $F(m_i, m_{\text{ref}})$, called the fractionation factor, is a function of the atomic masses of the ith and reference isotopes, m_i and m_{ref} respectively.

There are several different empirical fractionation laws which all follow this general form. They each use different functions to model mass dependent fractionation. The fractionation factor is defined differently in each model. The simplest form is the linear fractionation law:

$$F(m_i, m_{\text{ref}}) = (1 + f * (m_i - m_{\text{ref}})) \tag{3.2}$$

where f is the linear fractionation factor, reported in permille (parts per thousand). Using this law, if for example the ^{96}Mo/^{95}Mo ratio increased by 1 ‰, then the ^{97}Mo/^{95}Mo ratio would increase by 2 ‰, while the ^{92}Mo/^{95}Mo would decrease by -3 ‰. This law provides a simple approximation of real world fractionation and can be accurate within 0.2 ‰. A more

accurate fractionation model is called the exponential law, or Russell's law[36]:

$$F(m_i, m_{\text{ref}}) = \left(\frac{m_i}{m_{\text{ref}}}\right)^{\alpha} \tag{3.3}$$

where α is the fractionation exponent. This was originally applied to TIMS measurements, and it is now the most common model used for ICP-MS measurements. It is generally accepted as giving the best representation of the instrumental mass bias that occurs during ICP-MS measurements[35], based on comparison of predicted and measured fractionation. Determining which fractionation law applies best to the instrument is necessary in order to use the double-spike technique to correct for instrumental mass bias.

3.4 Double-spike technique

The double-spike technique, originally published by Dodson in 1963[37] and developed further by R.D. Russell in 1971[38], is used to correct for instrumental mass fractionation by mixing the sample being measured with a calibrated double-spike, also known as a tracer. The double-spike is composed of two single spikes which are materials that have been highly enriched (typically >95 %) in a single isotope. Figure 3.1 compares the natural composition of molybdenum to that of the double-spike. The calculations described later in this chapter require three isotope ratios, so the technique can only be applied to elements with at least four isotopes including three isotopes for the three numerators and one isotope for the denominator of the ratios. Figure 3.2 outlines the basic process of double-spiking.

It is not possible to directly measure the absolute isotopic composition of the sample and sample-spike mixture. The measured isotopic composition will have some mass bias, represented by α and β for the sample and sample-spike mixture respectively. If the double-spike is calibrated (described in section 3.5), these fractionation factors can be determined and corrected for, as described below.

The isotope ratios of the mixture are defined by the following equation[17]:

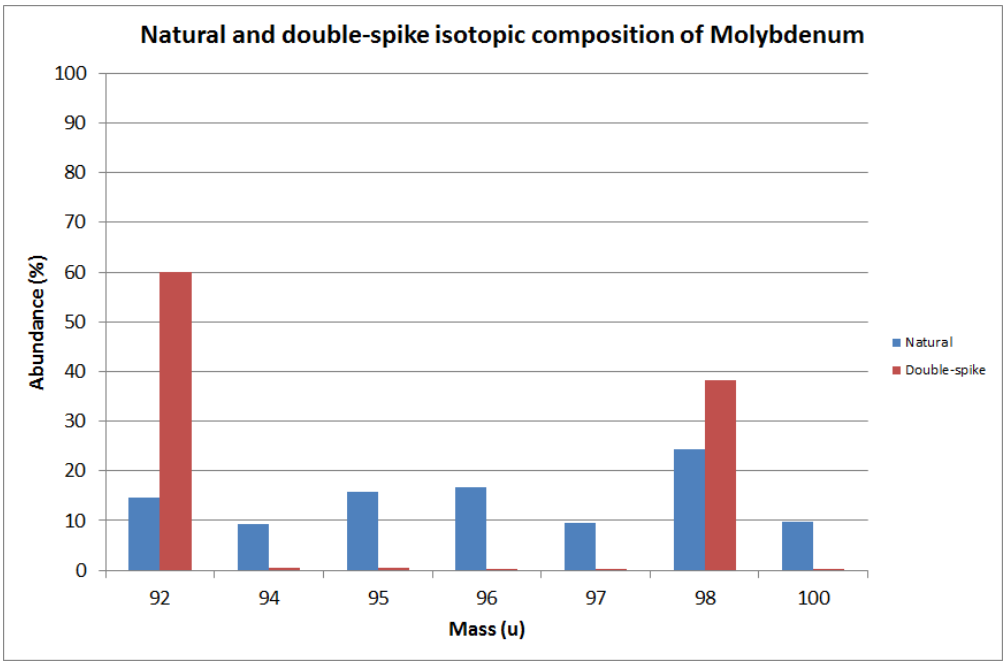

Figure 3.1: Comparison of the molybdenum isotopic composition in natural samples and the double-spike.

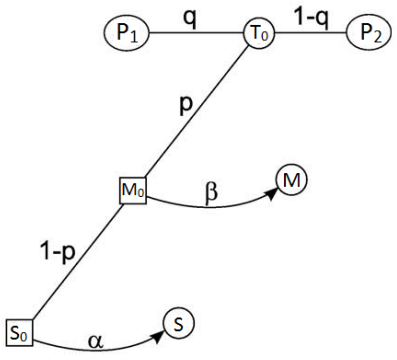

Figure 3.2: This figure, modified from Rudge 2009[17], shows the mixture of the double-spike T_0, which is made up of primary spikes P_1 and P_2, with sample S_0 to form M_0. The mixture consists of a proportion per mole p of the double-spike and $(1-p)$ of the sample. Measurements of the mixture and sample are fractionated with fractionation exponents β and α respectively resulting in M and S.

$$M_{0,i} = S_{0,i}\lambda + T_{0,i}(1-\lambda) \tag{3.4}$$

where $M_{0,i}$, $S_{0,i}$ and $T_{0,i}$ are the ith true ratios of the mixture, standard and double-spike respectively, and λ is related to the molar proportion of spike in the mixture as follows:

$$p = \left(1 + \frac{1-\lambda}{\lambda}\frac{\sum_i S_{0,i}}{\sum_i T_{0,i}}\right)^{-1} \tag{3.5}$$

where p is the molar proportion of spike. The sums are taken over all isotope ratios including the unitary ratio (i = ref). While the double-spike is assumed to be calibrated, the measurements of the unspiked sample and the sample-spike mixture are not resulting in isotopic compositions that are fractionated from their true values due to instrumental mass bias:

$$S_{0,i} = S_i \left(\frac{m_i}{m_{\text{ref}}}\right)^{-\alpha} \tag{3.6}$$

$$M_{0,i} = M_i \left(\frac{m_i}{m_{\text{ref}}}\right)^{-\beta} \tag{3.7}$$

Note that the exponents are now negative, as these equations are the inverse of Eq. 3.1 with Eq. 3.2. Combining equations 3.4, 3.6 and 3.7 we are left with the equation:

$$M_i \left(\frac{m_i}{m_{\text{ref}}}\right)^{-\beta} = S_i \left(\frac{m_i}{m_{\text{ref}}}\right)^{-\alpha} \lambda + T_{0,i}(1-\lambda) \tag{3.8}$$

This equation has three unknowns: α, β and λ. By using three different isotope ratios, we have three equations, with three unknowns. Although this system of equations cannot be solved analytically, it can can be determined using numerical techniques, such as the FindRoot command built into *Wolfram Mathematica*. Once the system is solved, α is applied to Equation 3.6 to determine the true isotopic composition. Equation 3.5 can also be used to determine proportion of spike in the mixture, which can then be applied to determine the amount of molybdenum from the sample if it is unknown.

Uncertainty propagation is done using Monte Carlo simulation by randomly choosing values from a normal distribution centered about each input value with a standard deviation equal to the uncertainty of the input value. This is done for all of the input values, and the uncertainties are determined after a sufficient number of iterations such that the results converge (n=1000). This technique ensures all sources of uncertainty are fully accounted for.

3.5 Double-spike calibration

In order for the double-spike method to be used to determine an absolute isotopic composition, the double-spike must be properly calibrated. This means knowing the absolute isotopic composition of the double-spike after it has been corrected for isotopic fractionation. The technique used by Wieser and De Laeter[1] begins with the preparation of several double-spikes, each with differing proportions of the primary spikes. These mixtures are defined similarly to Equation 3.8, except no ratios are calibrated:

$$T_i \left(\frac{m_i}{m_{\text{ref}}}\right)^{-\beta} = P1_i \left(\frac{m_i}{m_{\text{ref}}}\right)^{-\alpha} \lambda + P2_i \left(\frac{m_i}{m_{\text{ref}}}\right)^{-\gamma} (\lambda - 1) \tag{3.9}$$

where $P1$ and $P2$ are each of the primary spikes. After applying Equation 3.5 this equation can be solved for λ to give:

$$\lambda = \left(1 + \frac{1-p}{p} \frac{\sum_i P2_{0,i}}{\sum_i P1_{0,i}}\right)^{-1} \tag{3.10}$$

where p is the molar proportion of spike $P1$ in the mixture. p is related to the number of moles of each primary spike used:

$$p = \frac{N_{P1}}{N_{P1} + N_{P2}} \tag{3.11}$$

The mass of each spike added to the mixture is measured gravimetrically. The number of moles of each primary spike used is related to the mass(g) of primary spike by:

$$N_{P1} = \frac{\mu_{\mathrm{P1}} * \sum_i (P1_{0,i})}{N_A \sum_i (P1_{0,i} * m_i)} \tag{3.12}$$

where μ_{P1} is the mass (g) of spike used, m_i is the atomic mass (Da) if the ith isotope, and N_A is the Avogadro constant. $P1_{0,i}$ is related to $P1_i$ by:

$$P1_{0,i} = P1_i \left(\frac{m_i}{m_{\mathrm{ref}}} \right)^{-\alpha} \tag{3.13}$$

and similarly for P2.

By measuring the mass of each primary spike precisely in each double-spike mixture, we control the variable p and therefore λ. However, equation 3.9 is still left with three unknowns: α, β and γ. These fractionation exponents will be different as the instrumental mass bias changes over time between measurements of samples. By monitoring the change in mass bias over time, it is possible to determine the difference between the fractionation factors α, β and γ, and to correct the isotope abundance ratios to have the same fractionation factors, $\alpha = \beta = \gamma$. This is done using standard-sample bracketing which is described in the next section.

We are now left with a single equation with just one unknown, α. Using the ratio of P1's spiked isotope to P2's spiked isotope for $P1$, $P2$ and T, equation 3.9 can be solved numerically, giving us α and allowing us to determine the absolute composition of the double-spike:

$$T_{0,i} = T_i \left(\frac{m_i}{m_{\mathrm{ref}}} \right)^{-\alpha} \tag{3.14}$$

3.6 Standard-sample bracketing

As described in section 3.5, it is necessary to monitor the instrument fractionation during each separate measurement to calibrate the double-spike isotopic composition. The mass bias of the instrument can change between individual measurements of samples and from day to

day between measurement sessions. This drift can be quantified by measuring a laboratory reference material, and comparing the measured ratios to a previous measurement of the same material. This tells us how much the mass bias has changed since the preceding measurement. Standard-sample bracketing is done by measuring a laboratory standard before and after measuring each sample. Thus, we can predict the relative instrumental fractionation during the measurement of the sample. The arbitrary starting value can be determined from any measurement of the standard, and is used to set a common reference point. Correcting for the mass bias drift to this reference point results in all instrumental fractionation factors being equal, though not equal to zero. Let $S0_i$ be the set of measured isotope abundance ratios of our arbitrary starting value for the standard, while $S1_i$ and $S2_i$ are the measured isotope ratios of the standard measured before and after the measurement of the sample isotope ratios, which we will call Q_i. The two bracketing standard measurements will be fractionated relative to the starting value with fractionation exponents α_1 and α_2. Eq. 3.6 is solved for α:

$$\alpha_1 = \frac{1}{n} \sum_i \left(\frac{\ln\left(\frac{S1_i}{S0_i}\right)}{\ln\left(\frac{m_i}{m_{\text{ref}}}\right)} \right) \tag{3.15}$$

where n is the number of isotopes for the element, and similarly for α_2. The fractionation exponent of the sample, α_Q, can then be determined by assuming the fractionation drifts linearly in time between the bracketing standards (Section 6.4 demonstrates this assumption to accurate to within 0.08 ‰):

$$\alpha_Q = \alpha_1 + \left(\frac{t_Q - t_1}{t_2 - t_1} \right) (\alpha_2 - \alpha_1) \tag{3.16}$$

where t_1, t_2 and t_Q are the times at which each measurement was taken. This brings each sample measurement back to the same relative fractionation as the arbitrary starting value.

To demonstrate this, suppose we have measured the double-spike and a primary spike at different times. Each would have a different instrumental fractionation exponent, α and β:

$$T_{0,i} = T_i \left(\frac{m_i}{m_{\text{ref}}} \right)^{-\alpha} = T_i \left(\frac{m_i}{m_{\text{ref}}} \right)^{-(\alpha_0 + \alpha_T)} \tag{3.17}$$

$$P1_{0,i} = P1_i \left(\frac{m_i}{m_{\text{ref}}} \right)^{-\beta} = P1_i \left(\frac{m_i}{m_{\text{ref}}} \right)^{-(\alpha_0 + \alpha_{P1})} \tag{3.18}$$

By correcting for the relative fractionations α_T and α_{P1}, we are left with two measurements with the same fractionation factor, α_0.

3.7 Conclusion

Isotopic fractionation is a shift in the isotopic composition of an element that results from mass dependent processes. Although the isotopic fractionation that occurs in nature is the subject of much research, it is important to characterize the fractionation that occurs during the measurement process. The exponential law best models this fractionation, and is used with the double-spike technique to quantify and correct for instrumental mass bias. By accurately preparing gravimetric mixtures of single isotope spikes, and combining the mixtures with standard reference materials, the absolute isotopic composition of the double-spike can be determined to fully calibrate the double-spike. Standard-sample bracketing is an important tool used to correct for changes in instrumental mass bias between measurements. Figure 3.3 summarizes the process described in this chapter.

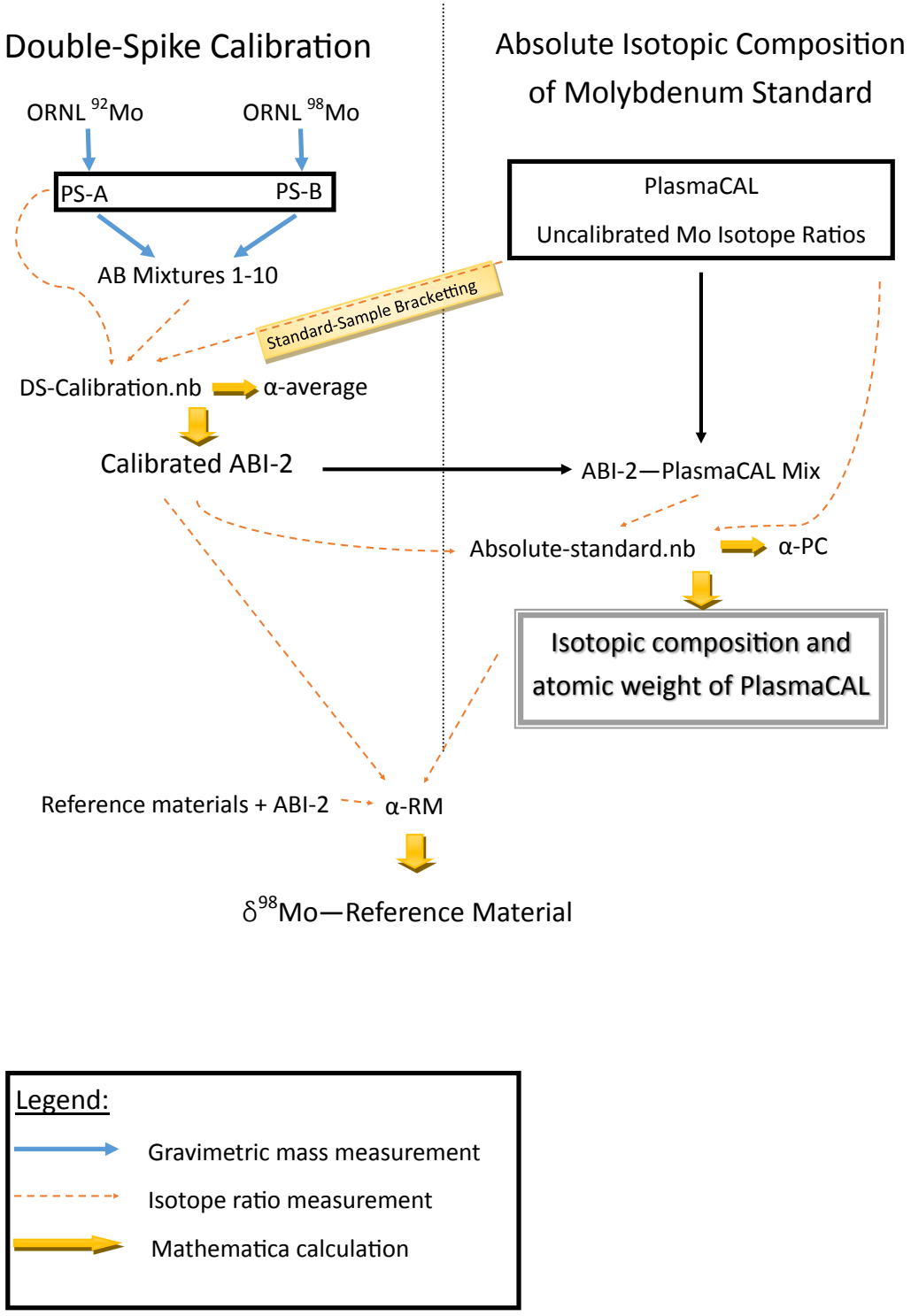

Figure 3.3: Flow chart visualizing the process described in Chapter 3. The left half of the chart is applied to the preparation of the double spike in Chapter 4, and the right half is applied to the measurement of the PlasmaCal reference material in Chapter 5. Finally, these are put together at the bottom of the chart to measure various other reference materials at the end of Chapter 5.

Chapter 4

Double-spike calibration

4.1 Introduction

In this chapter I will discuss laboratory procedures for preparing and calibrating the molybdenum double-spikes. I detail the procedures used to weigh and mix the pure metal molybdenum spike materials. This is followed by an overview of the operation of the Neptune MC-ICP-MS. Finally, I will describe the results and analysis used to calibrate the molybdenum double-spike.

4.2 Preparation of primary spikes

An isotope spike is a sample of an element that has been highly enriched in a single isotope. The isotope spikes which are purchased typically as a pure metal powder must be dissolved into a solution for use in mass spectrometry. The ^{92}Mo and ^{98}Mo primary spikes, labeled PSA and PSB respectively, were prepared from Oak Ridge National Laboratory (ORNL) molybdenum metals individually enriched in ^{92}Mo (Series ND, Batch 159390) and ^{98}Mo (Series LB, Batch 134590). The metal powder spikes were each transferred into separate PFA containers and dissolved with 2 mL of concentrated Seastar Baseline HCl (34 - 37 %) and 1 mL HNO_3 (67 - 70 %). The solutions were then diluted to the required concentration with 3% HNO_3. The masses of the empty PFA bottles, the bottles with the spikes added, and the bottles with the acids added were each taken by making 10 consecutive measurements using a Mettler-Toledo AT201 milligram balance. The masses of the glass bottles the spikes came in before and after the spike was removed were also measured, to confirm the amount of spike removed from the glass bottle was equal to the amount added to the PFA bottle.

The means and standard deviations of these masses are reported in Table 4.1, along with the calculated amounts of the spikes and acid used for each mixture.

	PSA (^{92}Mo) - Mass (g)	PSB (^{98}Mo) - Mass (g)
Empty PFA Bottle	67.5911(4)	67.8327(15)
+ Isotope Spike	67.7266(3)	68.017(2)
+ 3% HNO_3	185.294 29(7)	187.7049(2)
Glass bottle before	8.223 66(2)	8.378 30(4)
Glass bottle after	8.081 54(5)	8.185 55(8)
$mass_{92}$ added	0.1355(5)	0.185(3)
$mass_{92}$ removed	0.142 13(5)	0.192 76(9)
$mass_{soln}$	117.7033(4)	119.8722(15)

Table 4.1: Masses measured during preparation of primary spikes (PSA and PSB). For each value, the standard deviation of 10 consecutive measurements is reported at 1 s.d.

There was a 5 % difference between the amount of molybdenum removed from the glass bottles and the amount added to the PFA containers. The molybdenum was emptied directly from one container to the other, so no molybdenum should have been lost. It was observed that the PFA bottles could develop an electro-static charge. The effect of static electricity could be felt while handling the bottles. Also, when brought near but not in contact with the mass balance, the balance reading changed by as much as several milligrams. Further, the static can attract dust or other aerosols, also changing the measured mass by up to several milligrams. This resulted in less precision and inaccurate mass measurements. The static electricity problem was observed to not affect the glass bottles, so the masses of the spike removed from the glass bottles were taken as correct. This effect is studied and detailed in Chapter 6. The concentrations of molybdenum in the primary spikes is presented in Table 4.2.

Spike	[Mo] (mg/g)
PSA	1.2075(4)
PSB	1.6080(8)

Table 4.2: Primary spike concentrations determined using the masses of each spike removed from the original glass bottles along with the total mass of solution in the PFA bottles.

4.3 Preparation of double-spikes

In order to calibrate the double-spikes using the method outlined in Chapter 3, a set of mixtures were made containing different proportions of primary spikes A (^{92}Mo) and B (^{98}Mo). Two sets of five mixtures were prepared by pipetting the desired amount of each primary spike (PSA and PSB) into clean Teflon containers. The masses of the empty bottles and the bottles with each spike added were measured 10 times, and the calculated mass of each spike in each mixture is reported in Table 4.3. Unlike the preparation of the primary spikes, the mass of the source bottles were not used since some solution can remain in the pipette tip.

Mixture	mass_{PSA}(g)	mass_{PSB}(g)
ABI-1	13.018(5)	12.415(3)
ABI-2	12.667(6)	6.330(4)
ABI-3	12.556(9)	3.1005(8)
ABI-4	12.464(10)	1.6459(5)
ABI-5	15.321(5)	1.036(2)
ABII-1	9.7298(6)	6.0208(8)
ABII-2	6.7038(5)	6.0554(5)
ABII-3	2.9992(9)	6.0110(10)
ABII-4	1.5121(5)	6.0149(6)
ABII-5	0.7103(9)	6.0787(9)

Table 4.3: Masses of each primary spiked used in each mixture. Amounts were chosen to include PSA to PSB molybdenum mass ratios approximately between 10:1 and 1:10.

Ten different mixtures were prepared in order to improve the accuracy and relative uncertainty of the calibration. An individual mixture may be subject to offsets during the mass measurements and by creating ten different mixtures, the random error can be assessed. By varying the proportions of each spike in the mixtures, it is possible to choose the double-spike with the optimum ratio of PSA to PSB, which will be discussed later.

4.4 MC-ICP-MS Operation

All isotopic composition measurements were taken using a Thermo Scientific Neptune MC-ICP-MS. Multiple samples can be measured in succession automatically using the Elemental Scientific auto-sampler. The sample is introduced to the plasma through a Glass Expansion nebulizer (100 μL/min) and cyclonic spray chamber (20 mL). Excess liquid is removed from the spray chamber with a peristaltic pump. Table 4.4 outlines the operating conditions of the plasma. The sample and auxiliary gas flow, the torch position, and the focus settings were optimized to ensure maximum intensity, good peak shape, and good stability. A typical peak scan is shown in Figure 4.1.

Parameter	Setting
RF Power	1200 W
Cool gas flow	16 l/min
Aux gas flow	$\sim$1 l/min
Sample gas	$\sim$1 l/min
Sample uptake rate	100 μl/min

Table 4.4: MC-ICP-MS operating parameters

Eight Faraday cups were used to simultaneously collect the seven isotopes of molybdenum, along with ^{91}Zr. This allowed for the constant measurement of $^{91}Zr^{+}$ to monitor the isobaric interferences on ^{92}Mo and ^{94}Mo. ^{91}Zr was collected on cup L4 with a 10^{12} Ω resistor, while the rest are collected on cups L3-H3 each with 10^{11} Ω resistors. Amplifier gain calibration was performed at least once per week.

A typical measurement session began by allowing the instrument to warm up for a minimum of one hour by aspirating 3% HNO_3 into the spray chamber and plasma. During this period, the plasma and mass bias can stabilize prior to taking measurements. Once the instrument is warmed up, PlasmaCal Mo solution is used to tune the instrument. This includes optimizing the operating parameters and focus settings for good peak shape, stability and intensity, as well as collecting a set of Mo isotope abundance ratios to check that the ratios are within the accepted range of values. The intensity of $^{98}Mo^{+}$ was required to be at least

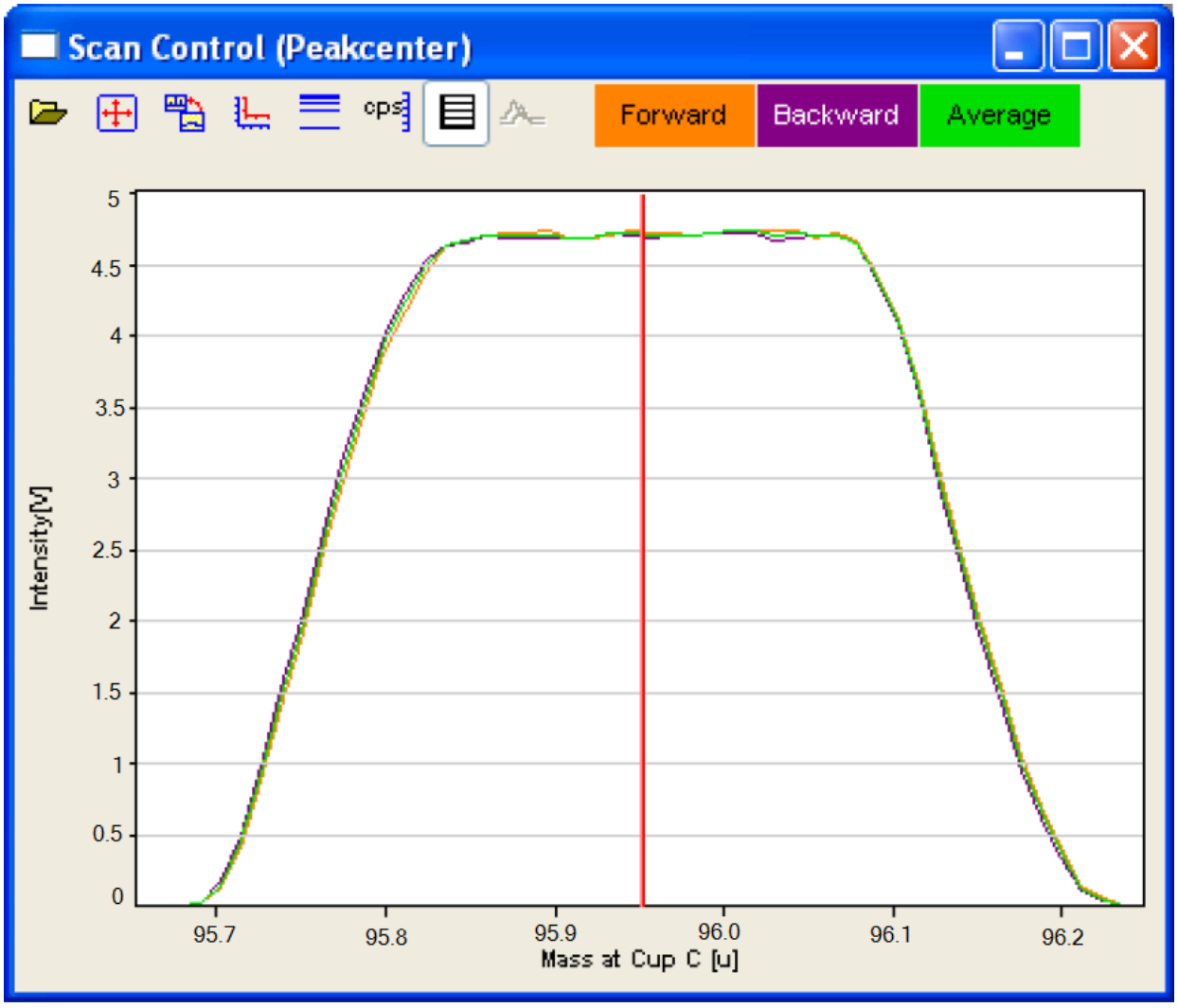

Figure 4.1: A typical peak scan for ^{96}Mo. The flat and wide top ensures stable measurement of the ion current.

2 V, and the normalized isotope abundance ratios were required to have an uncertainty less than 100 ppm. Measurement blanks were always monitored by measuring freshly prepared 3% HNO_3 by performing a mass scan on the SEM from mass 89 to 101, or by measuring a set of ratios using the same method as for samples. The concentration of molybdenum in all samples is approximately 200 ppb, though it can vary from 50 ppb to 2000 ppb in special cases.

The routine, or method, used for each measurement was as follows. First a peak centering on mass ^{98}Mo was performed, followed by a measurement of the electronic baseline by defocussing the ion beam. Next, seven blocks of 10-20 measurement cycles were performed. Each cycle measured the intensity measured at each cup averaged over 8.134 s. These intensities were converted to isotope ratios in the Data Evaluation software from the Neptune Multicollector software version 3.2.

This method can be executed for a set of samples automatically using the Neptune's Sequence Editor. A typical sequence will include several measurements of the PlasmaCal solution for standard-sample bracketing (see section 3.6). After each measurement, a minimum 60 s wash is performed with 3% HNO_3 to remove the residual molybdenum and other material from the nebulizer and spray chamber, followed by a measurement of the background in clean 3 % HNO_3. Although this second step is not necessary, it assists in monitoring the background signal intensities, which will increase over the course of a session.

Offline data analysis included mass bias drift correction and background correction. The measured background intensities are subtracted from the measured ratios using the following equation with an example for ^{98}Mo/^{95}Mo:

$$R_{i,\mathrm{bc}} = \frac{R_{i,s} I_{\mathrm{ref},s} - I_{i,b}}{I_{\mathrm{ref},s} - I_{\mathrm{ref},b}} \tag{4.1}$$

$$\left(\frac{^{98}\mathrm{Mo}}{^{95}\mathrm{Mo}}\right)_{\mathrm{bc}} = \frac{\left(\frac{^{98}\mathrm{Mo}}{^{95}\mathrm{Mo}}\right)_s \mathrm{I95}_s - \mathrm{I98}_b}{\mathrm{I95}_s - \mathrm{I95}_b} \tag{4.2}$$

where $R_{i,\mathrm{bc}}$ is the background corrected ratio, $I_{\mathrm{ref},s}$ and $I_{\mathrm{ref},b}$ are the intensities of the reference isotope measured for the sample and blank respectively, and $I_{i,b}$ is the intensity of the ith isotope of the blank. The blank correction cannot change the ratio by more than 100 ppm, or else the ratio will not be accepted.

4.5 Measurement of PlasmaCal

The internal standard used in the laboratory is *SCP Science PlasmaCAL Standard - Molybdenum, Lot # SC9306057* (PlasmaCal) with a stock concentration of 10 000 μg/mL. This is an internationally available reference material which is traceable to the NIST molybdenum concentration standard (SRM 3134). The concentration of SRM 3134 is certified by NIST, however the isotopic composition is not. The first step is to establish an unnormalized isotopic composition as a common reference value. Table 4.5 shows the results of seven consecutive isotopic composition measurements made on February 7, 2011 of the PlasmaCal standard. Internal precisions for all measurements are ∼10 ppm (1sd) and are no higher than 20 ppm.

Run #	95 (V)	92/95	94/95	96/95	97/95	98/95	100/95
1	1.14004	0.880190	0.569895	1.066460	0.622328	1.601611	0.661886
2	1.18838	0.879523	0.569752	1.066724	0.622649	1.602818	0.662699
3	1.21195	0.878873	0.569613	1.066994	0.622958	1.603998	0.663520
4	1.21995	0.878635	0.569557	1.067085	0.623069	1.604466	0.663837
5	1.22284	0.878466	0.569527	1.067156	0.623136	1.604721	0.664006
6	1.22976	0.878646	0.569571	1.067078	0.623064	1.604419	0.663788
7	1.23056	0.878440	0.569513	1.067148	0.623142	1.604764	0.664043

Table 4.5: Unnormalized results with background correction for seven consecutive measurements of PlasmaCal taken on February 7, 2011.

The ratios varied substantially over the course of the measurement set as the mass bias drifted. To correct for the drift in mass bias over the course of a measurement session, it is common to normalize the ratios by performing a mass bias correction based on single isotope ratio. However, this necessarily eliminates the uncertainty in that ratio, and transfers it to

the other ratios. All ratios are fluctuating, so it is important to preserve the uncertainty in each isotope abundance ratio measurement and not transfer a single ratios uncertainty to the other ratios. This was done by calculating the fractionation exponent α for each isotope ratio compared to the first run and taking the average α of all six ratios:

$$\alpha_j = \frac{1}{6}\sum_i \left(\frac{\ln\left(\frac{RJ_i}{R1_i}\right)}{\ln\left(\frac{m_i}{m_{\text{ref}}}\right)} \right) \tag{4.3}$$

where α_j is the average fractionation exponent of the jth run, RJ_i and R1_i are the ith measured ratios of the jth run and first run respectively, and m_i and m_{ref} are the are the isotopic masses of the ith and reference isotopes respectively. This average α is then used to correct for the internal mass bias drift:

$$RJ_{i,c} = RJ_i \left(\frac{m_i}{m_{\text{ref}}} \right)^{-\alpha_j} \tag{4.4}$$

where $RJ_{i,c}$ is the ith internal mass bias corrected ratio for run j. Table 4.6 shows the average α's.

Run #	α
2	0.0240(4)
3	0.0476(7)
4	0.0564(9)
5	0.0619(6)
6	0.0554(11)
7	0.0627(7)

Table 4.6: Average α from Table 4.5 calculated using Equation 4.3.

Table 4.7 shows the internally normalized ratios for the seven measurements of PlasmaCal. After correcting for the mass bias drift, the external precision for each isotope ratio was determined for this measurement session to be 5-20 ppm. The average isotope ratios were used with standard-sample bracketing for all further internal normalization.

Run #	92/95	94/95	96/95	97/95	98/95	100/95
1	0.880190	0.569895	1.066460	0.622328	1.601611	0.661886
2	0.880200	0.569897	1.066456	0.622338	1.601622	0.661883
3	0.880217	0.569900	1.066463	0.622340	1.601623	0.661899
4	0.880229	0.569898	1.066455	0.622336	1.601651	0.661916
5	0.880214	0.569900	1.066465	0.622333	1.601634	0.661899
6	0.880212	0.569906	1.066459	0.622344	1.601654	0.661901
7	0.880210	0.569892	1.066448	0.622328	1.601637	0.661908
Mean	0.880210(12)	0.569898(4)	1.066458(6)	0.622335(6)	1.601633(16)	0.661899(12)

Table 4.7: Mass bias drift corrected results for seven consecutive measurements of PlasmaCal. Uncertainties are reported at 1 s.d.

4.6 Measurement of primary spikes

Now that the unnormalized isotope amount ratios of the lab standard have been determined, it is possible to measure the isotopic composition of the rest of the calibration materials beginning with each of the primary spikes. The primary spikes present a unique challenge as they are highly enriched in a single isotope. When the molybdenum concentration is 200 ppb, such that the spiked isotope is near the maximum measurable intensity (<50 V), the unspiked isotopes will have intensities that are 170-520x smaller (as low as 50 mV). The baselines are greater than 0.1 mV, and the backgrounds can be up to 0.5 mV leading to interferences up to 1 % of the signal intensity. This problem was resolved by making two separate sets of measurements for each spike. The first was a measurement of the spike with a normal concentration (∼200 ppb), while the second was a measurement of the spike with a much higher concentration spike (2000 ppb). During the second measurement, the spiked isotope's ion beam could damage the Faraday cup and amplifiers, so the Faraday cup was moved to not collect the spiked isotope. This allowed for a precise determination of the major and minor isotope ratios.

Table 4.8 shows the measured ratios of the ^{92}Mo spike, primary spike A (PSA), and the ^{98}Mo spike, primary spike B (PSB). The results from the high concentration measurements were used for the unspiked isotopes, while the results from low concentration measurement were used for the spiked isotope.

Spike	92/95	94/95	96/95	97/95	98/95	100/95	N
PSA Lo	172.408(26)	1.29354(5)	0.69155(2)	0.34538(5)	0.816(10)	0.6015(3)	11
PSA Hi	-	1.293911(15)	0.691418(7)	0.345321(4)	0.8474(2)	0.601226(15)	5
PSB Lo	0.57640(25)	0.45892(17)	1.64387(10)	2.81681(19)	520.60(4)	1.58801(29)	11
PSB Hi	0.576574(23)	0.459239(11)	1.64420(3)	2.81741(8)	-	1.58882(9)	5

Table 4.8: Mass bias drift corrected isotope ratios for PSA and PSB. Each measurement was repeated N times. The first run is normalized using standard-sample bracketing (see Chapter 3.5). The consecutive runs are normalized to the first run as was done for the lab standard. Uncertainties are reported at 1 s.d.

4.7 Measurement of the molybdenum isotopic composition of double-spike mixtures

The isotopic composition of the double-spike mixtures were measured over the course of several measurement sessions. Mass bias drift was corrected using standard-sample bracketing. For the calibration, only the ^{98}Mo/^{92}Mo ratios were required, however, the remaining ratios are necessary when using the double-spike technique to measure the isotopic composition of samples. Table 4.9 contains the measured ratios for each of the mixtures and Table 4.7 contains the $^{98/92}$Mo ratio for each mixture.

Spike Mixture	92/95	94/95	96/95	97/95	98/95	100/95
ABI-1	119.98(3)	1.039 65(9)	0.9825(6)	1.097 05(2)	158.93(4)	0.9006(4)
ABI-2	140.24(4)	1.138 42(13)	0.8703(4)	0.806 056(9)	97.74(2)	0.7846(4)
ABI-3	154.78(5)	1.208 94(13)	0.7893(4)	0.596 651(13)	53.696(14)	0.7007(4)
ABI-4	162.41(5)	1.246 16(14)	0.7467(4)	0.486 396(11)	30.534(8)	0.6566(4)
ABI-5	167.15(5)	1.269 05(14)	0.7205(4)	0.418 492(9)	16.257(4)	0.6295(3)
ABII-1	134.40(4)	1.109 92(12)	0.9030(5)	0.891 154(20)	115.66(3)	0.8175(4)
ABII-2	121.98(4)	1.050 06(12)	0.9721(6)	1.070 062(24)	153.24(4)	0.8891(5)
ABII-3	90.04(3)	0.894 73(10)	1.1489(7)	1.528 03(3)	249.50(7)	1.0716(6)
ABII-4	61.442(19)	0.756 26(8)	1.3081(7)	1.939 66(4)	336.05(9)	1.2359(7)
ABII-5	35.327(11)	0.629 30(7)	1.4525(8)	2.314 14(5)	414.76(11)	1.3852(8)

Table 4.9: Isotope ratios for spike mixtures. Results are normalized using standard-sample bracketing. Uncertainties for ABI-1 and ABI-2 estimated as the range of two replicate analyses. The remaining mixtures were only measured once, so their uncertainty is estimated as the maximum relative uncertainty of the respective ratios for ABI-1 and ABI-2.

Spike	98/92
ABI 1	1.324 681(11)
ABI 2	0.696 95(7)
ABI 3	0.346 91(4)
ABI 4	0.188 002(20)
ABI 5	0.097 261(10)
ABII-1	0.860 60(9)
ABII-2	1.256 26(13)
ABII-3	2.7710(3)
ABII-4	5.4694(6)
ABII-5	11.7407(12)

Table 4.10: ^{98}Mo/^{92}Mo ratios calculated from isotope ratios in Table 4.9

4.8 Overall fractionation correction

Chapter 3 described the method used to determine the absolute isotopic composition of the double-spike and standard. The method described was implemented in *Mathematica*, and the results follow in Table 4.11. The code used is provided in Appendix 1.

Spike	α
ABI-1	1.451(20)
ABI-2	1.451(23)
ABI-3	1.447(22)
ABI-4	1.463(24)
ABI-5*	1.210(40)
ABII-1	1.433(19)
ABII-2	1.469(19)
ABII-3	1.435(20)
ABII-4	1.407(19)
ABII-5*	1.492(28)
Mean	1.444(28)

Table 4.11: List of calculated α's. *The α determined from the fifth mixture in each set was well outside the range of the other values and was not used for the calculation of the mean. Uncertainty was determined by Monte Carlo simulation with N=1000 iterations.

The α determined from the fifth mixture in each set was outside the range of the other values. This was most likely caused by a ∼10 mg offset in the measurement of the spike masses used to create the mixture which, as noted in Section 4.1, could have been caused by electrostatic charge on the PFA container which attracted dust and affected the milligram

balance measurement.

The mean α calculated can now be applied to the double-spike isotope amount ratios to determine their absolute isotopic compositions. ABI-2 was chosen as having the optimum proportion of ^{92}Mo and ^{98}Mo primary spikes based on the Rudge "Double-spike toolbox"[17], which gives a list of the optimal double-spikes depending on the isotopes used, based on the lowest predicted uncertainty. The absolute isotope ratios of ABI-2 are reported in Table 4.12. These ratios can now be used to determine the absolute isotopic composition of the reference materials.

Sample	92/95	94/95	96/95	97/95	98/95	100/95
ABI2	146.90(14)	1.1560(4)	0.8572(5)	0.7821(5)	93.44(8)	0.7285(10)

Table 4.12: Absolute isotope ratios for ABI2, calculated using mean α from Table 4.11. Uncertainty propagated from isotope ratio measurement uncertainty and uncertainty in α using Monte Carlo simulation.

4.9 Conclusion

The ^{92}Mo and ^{98}Mo primary spikes were prepared with accurate gravimetric measurements of the ORNL pure metal isotope spikes. These were mixed in different proportions to prepare ten double-spikes. The Neptune ICP-MS was used to measure an initial set of uncalibrated isotope amount ratios for the PlasmaCal standard. After a mass bias drift correction, the average ratios calculated from this set were used for standard-sample bracketing on the remaining measurements. The primary spikes' and double-spikes' isotope ratios were measured and the results were applied to the double-spike calibration algorithm to determine the total instrumental isotopic fractionation. The optimum double-spike, ABI-2, was fully calibrated by correcting for the total instrumental mass bias and can now be used to measure the absolute isotopic composition of the standard reference materials.

Chapter 5

Absolute isotopic composition of reference materials

5.1 Introduction

In this chapter I will discuss the measurement and calculation of the absolute isotopic composition of various synthetic and natural reference materials. I begin with a discussion of pure molybdenum samples and the calculation of their absolute isotopic compositions. Then I will discuss the application of the double-spike method to measuring natural reference materials obtained from the United States Geological Survey (USGS). This includes an overview of the chemistry required to prepare the samples for analysis.

5.2 Pure molybdenum reference materials

The variety of instruments used, measurement conditions, and analysis techniques can result in highly variable measurements between laboratories and within a laboratory between different sample measurements. Therefore, measurements of the isotopic composition of molybdenum in natural samples are always compared to the isotopic composition of a standard reference material[7]. This eliminates differences in mass bias between measurements, producing independent results which can be compared between laboratories. These reference materials are typically a pure molybdenum sample which ensures straight forward and accurate measurement, with minimal chemical preparation which can introduce contaminations or alter the isotopic composition. At this time, there is no internationally accepted standard for molybdenum[32], making it difficult to compare results published by different groups. It is therefore important to properly determine the isotopic composition of these reference materials and establish an internationally available standard for intercomparison. A fully

calibrated measurement of the absolute isotopic composition can also be used to determine the atomic weight of the element.

5.2.1 PlasmaCal molybdenum reference material

The method used to determine the fractionation correction necessary for samples and standards is described in Chapter 3. Equation 5.1 is used to determine α, the fractionation exponent.

$$M_i \left(\frac{m_i}{m_{\text{ref}}} \right)^{-\beta} = S_i \left(\frac{m_i}{m_{\text{ref}}} \right)^{-\alpha} \lambda + T_{0,i}(\lambda - 1) \tag{5.1}$$

where S_i, M_i and $T_{0,i}$ are the ith ratios of the sample, mixture, and calibrated double-spike respectively, m_i and m_{ref} are the isotopic masses of the ith and reference isotopes, α and β are the instrumental fractionation exponents of the sample and mixture, and λ is a proportionality factor related to the sample to spike ratio. In order to determine the absolute isotopic composition of the sample, this equation must be solved for α, β, and λ. α can then be used to correct for instrumental mass bias.

Two of the three required sets of ratios have already been determined in Chapter 4, the calibrated isotope ratios for the double-spike and the uncalibrated isotope ratios for our lab standard, which were measured and used for standard-sample bracketing. The third set of ratios requires a measurement of a mixture of the sample and double-spike.

When preparing the mixture of sample and double-spike, it was important to control the ratio of double-spike to sample. If there was too much double-spike, the unspiked isotopes would be difficult to measure, increasing the uncertainty. If there was too little double-spike, the spiked isotopes would be difficult to differentiate from the sample, also increasing the uncertainty. Figure 5.1 demonstrates this effect. This plot was generated by predicting the isotope ratios generated by mixing our double-spike and standard, and applying the three sets of ratios to the double-spike algorithm. Each of the ratios generated were varied

assuming two types of uncertainty: a random uncertainty of 100 ppm about the mean, and a random uncertainty due to background noise of up to 0.1 mV on each signal, assuming the sum total intensity for all isotope signals to be 10 V . This is similar to the types of uncertainty that would be encountered during a normal measurement. As seen, the optimal relative amount of double-spike is between 40% and 60% or around 1:1 sample to spike.

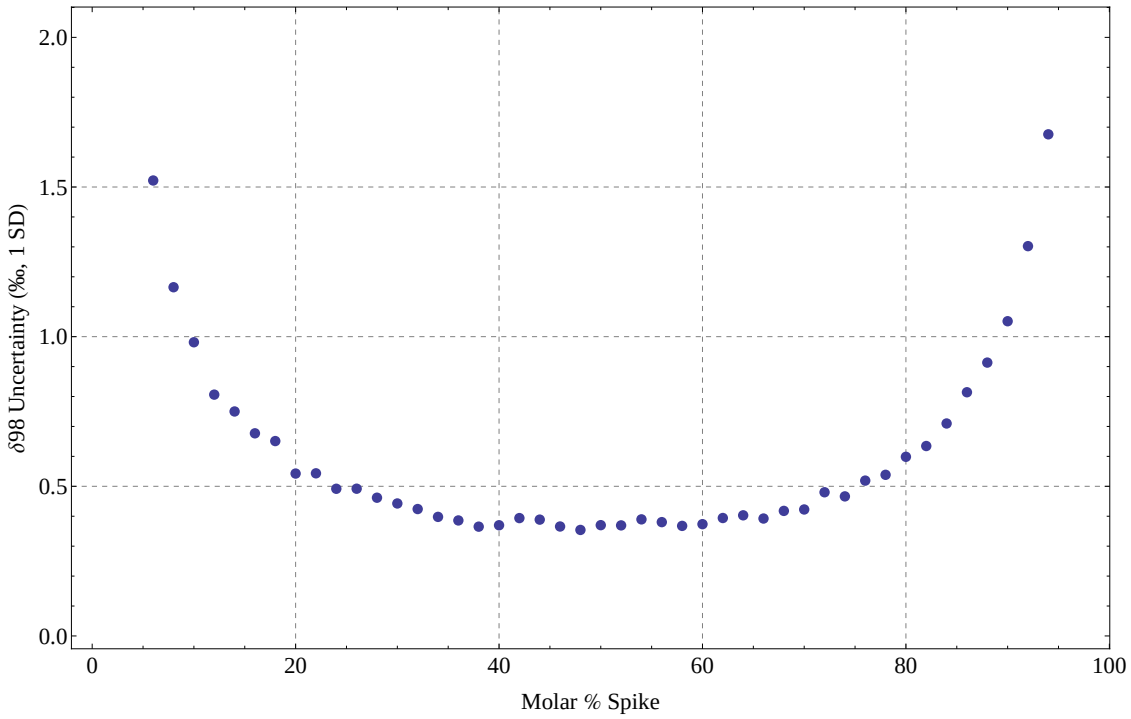

Figure 5.1: This plot shows how the uncertainty of the measured fractionation varies depending on the relative amount of spike used in the sample spike mixture.

Mixtures were prepared of the double-spike with several different widely available pure molybdenum reference materials, which were calibrated for molybdenum concentration only. These included *SCP Science PlasmaCAL Standard - Molybdenum*, which is used as our internal lab standard, *NIST SRM 3134 Molybdenum Standard Solution, Lot # 891307*, a certified molybdenum solution, and a solution of molybdenum that was prepared by dissolving a 99.993% spectroscopically pure metal rod *(Johnson-Matthey Chemicals Ltd., JMC 726, No. S-8555)*. The last solution was prepared at Curtin University, Western Australia, and was used in the most recent determination of the absolute isotopic composition

of molybdenum[1].

Several mixtures of PlasmaCal and spike were prepared with varying relative amounts of spike. This allowed us to confirm the precision over the 40% to 60% range. Each mixture was measured multiple times, and the results are reported in Table 5.1.

% Spike	α-94/95	α-96/95	α-97/95	α-100/95	N
42.0	1.414(4)	1.387(10)	1.4303(15)	1.418(5)	3
44.2	1.417(2)	1.385(19)	1.4320(2)	1.414(4)	2
48.9	1.417(9)	1.384(18)	1.4329(3)	1.417(7)	2
54.1	1.423(4)	1.387(16)	1.4327(9)	1.423(5)	3
59.1	1.423(5)	1.385(16)	1.4355(17)	1.422(3)	3
Average	1.419(6)	1.386(13)	1.4327(21)	1.419(5)	13

Table 5.1: Results for different mixtures of PlasmaCal and spike. α is calculated with the two spiked ratios(^{92}Mo/^{95}Mo and ^{98}Mo/^{95}Mo) and the third ratio as shown in the table. The uncertainty only includes the variation in N replicate analyses and not the uncertainty propagated from the double-spike calibration.

Calculation of α requires three isotope amount ratios, two of which must include the two spiked isotopes (ie. ^{92}Mo/^{95}Mo and ^{98}Mo/^{95}Mo), while the third can be chosen from the remaining ratios. When choosing the third ratio, it is important to choose one that is free from interferences. For this reason, the ^{94}Mo/^{95}Mo and ^{96}Mo/^{95}Mo ratio were not used, since there can be a $^{94}Zr^{+}$ interference and an unidentified mass-96 interference of up to 0.5 mV. In Table 5.1, we see very good precision for results obtained using ^{94}Mo/^{95}Mo, ^{97}Mo/^{95}Mo or ^{100}Mo/^{95}Mo as the third ratio. The best precision is obtained using ^{97}Mo/^{95}Mo as the third ratio, so it was used for all calculated results. It is important to note that since PlasmaCal was used as the internal lab standard for bracketing during the double-spike calibration, the fractionation exponent is expected to be the same as that calculated for the double-spike correction. The value obtained from the calibration was $\alpha = 1.444(28)$ which agrees within uncertainty of the α determined here of $\alpha = 1.4327(21)$. The uncertainty in Table 5.1 does not include the propagated uncertainty for the calibrated double-spike. This was intentional to highlight the different uncertainties for each chosen third isotope ratio, but the uncertainty of the calibrated double-spike is propagated in all future calculations.

5.2.2 Absolute isotopic composition and atomic weight of Plasma Cal molybdenum standard

The absolute isotopic composition of the Plasma Cal molybdenum reference material was determined by applying the correction factor obtained above using the ^{97}Mo/^{95}Mo value as the third ratio. The uncertainty in the α for the standard was expanded to include the uncertainty of the α for the double-spike of α =1.444(28) from Chapter 4. This uncertainty dominates the uncertainty in the α correction for the standard, and was propagated by Monte Carlo simulation: α-97=1.433(28). The isotopic composition is determined from the isotope ratios using the following equation:

$$P_i = \frac{R_i}{\sum_i R_i} \tag{5.2}$$

where the sum is over all ratios including the unitary ratio. The atomic weight is determined from the absolute isotopic composition as follows:

$$AW = \sum_i P_i * m_i \tag{5.3}$$

where m_i is the isotopic mass of the ith isotope.

By applying the correction factor to the unnormalized isotope ratios obtained in chapter 4, the absolute isotopic composition and atomic weight of the Plasma Cal molybdenum standard were determined. Table 5.2 shows the corrected isotope ratios for Plasma Cal, along with the absolute isotopic composition and atomic weight.

The measured atomic weight of 95.9508(16) is lower than the last reported value, though within uncertainty. The uncertainty is an order of magnitude less, and the atomic weight is closer to the previous reported values.

Isotope	Isotope abundance ratio (/^{95}Mo)	Isotopic Composition (%)	Previous best measured composition[1]	Representative composition (IUPAC)[2]
92	0.9217(8)	14.626(17)	14.525(15)	14.53(30)
94	0.57862(17)	9.182(5)	9.151(7)	9.15(9)
95	1(0)	15.869(5)	15.837(10)	15.84(11)
96	1.0506(4)	16.67(3)	16.672(19)	16.67(15)
97	0.6040(4)	9.585(3)	9.599(7)	9.60(14)
98	1.5318(13)	24.308(14)	24.391(18)	24.39(37)
100	0.6149(9)	9.758(11)	9.82(5)	9.82(31)
Atomic weight: 95.9508(16)			95.9602(23)	95.96(2)

Table 5.2: The isotope ratios, absolute isotopic composition and atomic weight of Plasma Cal molybdenum reference material. Uncertainties propagated from uncertainty in the measured isotope ratios and the uncertainty in the fractionation correction factor by Monte Carlo simulation. For comparison, the previous measured isotopic composition by Wieser and De Laeter[1] are reported, along with the IUPAC representative isotopic composition derived from the previous Wieser and De Laeter results with expanded uncertainty[2].

5.2.3 Relative composition of other pure molybdenum reference materials

When measuring natural or synthetic samples, the absolute isotopic composition is typically not reported. Instead the isotopic composition is compared to that of a laboratory standard, and the results are reported as a delta (δ) value in permille. For molybdenum, it is most common to report $\delta^{98/95}$Mo values, calculated as follows:

$$\delta^{98/95}\text{Mo} = \left(\frac{R0_{98,m}}{R0_{98,s}} - 1\right) * 1000 \tag{5.4}$$

where $\delta^{98/95}$Mo is the delta value in permille, $R0_{98,m}$ is the absolute ^{98}Mo/^{95}Mo ratio of the sample, free of any instrumental mass bias, and $R0_{98,s}$ is the absolute ^{98}Mo/^{95}Mo isotope abundance ratio of the standard. The sample is usually assumed to have undergone mass-dependent fractionation relative to the standard. This allows the isotopic composition of the sample to be equal to the isotopic composition of the standard with an added fractionation factor:

$$R0_{i,m} = R0_{i,s}\left(\frac{m_i}{m_{95}}\right)^{\alpha_{ms}} \tag{5.5}$$

where α_{ms} is the relative fractionation factor of the sample to the standard, and m_i and

m_{95} are the isotopic masses of ^{i}Mo and ^{95}Mo. If the sample has undergone mass independent fraction, such that the above equation does not hold true, a separate measurement of the isotopic composition prior to the sample being mixed with the spike is necessary, but this special case will not be discussed further since the selected samples have only undergone mass-dependent fractionation. The absolute isotope abundance ratios of the standard and sample can be related to an arbitrary measurement of the standard as follows:

$$R0_{98,m} = R_{98,i}\left(\frac{m_{98}}{m_{95}}\right)^{-\alpha_m} \tag{5.6}$$

$$R0_{98,s} = R_{98,i}\left(\frac{m_{98}}{m_{95}}\right)^{-\alpha_s} \tag{5.7}$$

where $R_{98,i}$ is the arbitrary isotope abundance ratio of the standard. α_m and α_s can be determined using the double-spike mixture calculation from section 5.2.1 by preparing mixtures of the sample and double spike, and standard and double spike, of which the latter has already been measured. If Equations 5.6 and 5.7 are substituted into Equation 5.4, we obtain the following:

$$\delta^{98/95}\text{Mo} = \left(\left(\frac{m_{98}}{m_{95}}\right)^{-(\alpha_m-\alpha_s)} - 1\right) * 1000 \tag{5.8}$$

The difference of the α's determined for the sample and standard is sufficient to calculate the delta value. If the isotopic composition of the standard is calibrated by correcting for instrumental mass bias, the value for α_s will be approximately equal 0, and we are left with the following:

$$\delta^{98/95}\text{Mo} = \left(\left(\frac{m_{98}}{m_{95}}\right)^{-\alpha_m} - 1\right) * 1000 \tag{5.9}$$

where α_m is determined from Equation 5.1 using the calibrated standard and double-spike ratios, with the measured ratios for the sample spike mixture.

Table 5.3 shows the determined delta values as compared to the calibrated PlasmaCal measurement for three synthetic molybdenum standards including a replicate of the PlasmaCal standard, the NIST SRM-3134 standard, and the molybdenum rod prepared at Curtin University. This was only a preliminary analysis done to estimate the range of fractionation for various pure molybdenum samples, so only one analysis was done for each sample. The uncertainty was estimated to be double that of the PlasmaCal measured in Table 5.1. It is important to control the sample-spike ratio as discussed earlier, so the mass % spike determined from the double-spike calculation is reported as well. The α determined for the PlasmaCal replicate was within uncertainty of $\alpha = 0$, which verifies the repeatability of the technique. The molybdenum rod had a small negative fractionation indicating a relative depletion of the heavy isotopes, and the NIST standard had a small positive fractionation indicating a relative enrichment of the heavy isotopes as compared to PlasmaCal. These fractionations could have been caused by the different chemical and physical processes used in the purification of the molybdenum, or by having different sources of molybdenum for the manufacturing of the standard material.

Sample	% Spike	α_m	$\delta^{98/95}$Mo (‰)
Curtin-Mo	44.3	0.010(4)	-0.32(14)
NIST-3134	43.3	-0.012(4)	0.37(14)
PlasmaCal	49.5	-0.003(4)	0.08(14)

Table 5.3: Delta values determined for three synthetic molybdenum samples. Uncertainties were predicted to be twice the uncertainty of the set of standard-spike measurements from Table 5.1.

5.3 Natural reference materials containing molybdenum

Four natural reference materials were obtained for analysis from the U.S. Geological Survey (USGS): BCR-1, basalt standard (no longer distributed); BCR-2, basalt standard; SDO-1, Devonian Ohio Shale; and SCO-1, Cody Shale. These standards all represent typical sample matrices which can be encountered in the laboratory, and are useful in demonstrating the

effectiveness of the technique in real world analyses, as well as demonstrating the range of natural variation in isotopic composition.

In order for natural samples to be analyzed, the molybdenum must be separated from the rest of the sample. This was achieved using ion exchange chemistry. This process can result in isotopic fractionation, therefore the double-spike was added at the start of the process. All fractionation that occurs due to chemistry will therefore be taken into account by the calculation, and the determined fractionation will reflect only the natural fractionation of the sample before the chemistry and analysis.

The sample was first digested in concentrated HCl (34 - 37%) to dissolve the matrix. This solution was separated from the solids by a centrifuge, then the double-spike was added and the solution was evaporated. The residue was dissolved in 4 M HCl for ion exchange. It is necessary to separate the molybdenum from compounds and complex matrices as they can disrupt the ionization of molybdenum in the mass spectrometer. It is also important to separate molybdenum from elements including zirconium and iron, as zirconium has isobaric interferences on molybdenum, and a high iron concentration can suppress the production and detection of molybdenum ions. This is done using ion exchange chemistry.

The ion exchange columns were first conditioned by following a series of steps shown in figure 5.2. The columns were first rinsed by passing through repeated aliquots of pure water obtained from the MilliQ water purification system (18.2 MΩ·cm). Different concentrations of HCl were passed through repeatedly to completely clean the resin. The sample solution in 4 M HCl was then passed through the conditioned anion resin column to separate the molybdenum from zirconium and most compounds. The first 10 mL of 4 M HCl contained the unwanted elements and compounds, and was discarded. The molybdenum was eluted from the column using 0.5 M HCl. The elution is then passed into the conditioned cation resin column, which separated the molybdenum from iron and the remaining elements. The molybdenum passes through freely, while the unwanted iron and other elements remain

ANION *1 cv ~ 2 mL*	
MQ H_2O	8 mL
4M HCl	6 mL
0.5M HCl	8 mL
4M HCl	4 mL
Sample in 4M HCl	S + 10 mL
Elute w/ 0.5M HCl	4 mL

CATION *1 cv ~ 2 mL*	
MQ H_2O	8 mL
4M HCl	4 mL
0.5M HCl	6 mL
Load in 0.5M HCl	S + 4 mL

Figure 5.2: From the worksheet used in the laboratory during ion exchange chemistry. The steps prior to the sample introduction are used to clean and condition the ion exchange columns.

attached to the column. The final elution was then evaporated and redissolved in 3 % HNO_3. This ensured a successful analysis in the mass spectrometer, free from isobaric interferences.

The natural samples had different concentrations of molybdenum, but we required the same amount of molybdenum for each analysis. Approximately 3 mL of the final solution was required for an analysis, with a concentration of 200 ppb Mo. Half of the molybdenum was from the sample, while the other half was from the spike. We therefore required ∼300 ng of molybdenum from the sample. Measurement blanks have been tested to be less than 1 ng and molybdenum recovery from the columns was typically greater than 90 %. Table 5.4 shows the molybdenum concentrations of each sample, along with the required amount of sample.

The analysis of BCR-1 and SCO-1 required large amounts of sample due to their low molybdenum concentration. The large amount of iron in these samples overloaded the ion exchange columns, which became discolored when these samples were introduced. Molyb-

Sample	[Mo] (μg/g)	Mass Required (mg)
BCR-1	1.6	187
BCR-2	248(17)	1.2
SDO-1	134(21)	2.2
SCO-1	1.4(0.2)	214

Table 5.4: Molybdenum concentrations and mass required for analysis of natural standard reference materials. Concentrations are as published by the USGS[3, 4, 5], except BCR-1[6].

denum and iron behave similarly on the anion column, so when the column was saturated with iron, both iron and molybdenum passed through the column before the recovery stage causing much of the molybdenum to be lost.

Sample	$\delta^{98/95}$Mo (‰)	N
BCR-1	14(17)	4
BCR-2	0.28(14)	4
SDO-1	1.5(5)	6
SCO-1	42(24)	4

Table 5.5: Delta values determined for natural standard reference materials containing molybdenum. Full digestion and ion exchange was performed for each replicate.

In Table 5.5, the determined delta values are reported. The results for the high concentration samples have acceptable precision and are within the range expected of natural molybdenum. BCR-2 has relatively more heavy molybdenum isotopes than the PlasmaCal reference material, while SDO-1 has more heavy molybdenum isotopes than BCR-2. However, the results for the low concentration samples have very high uncertainties for the measured delta value, and the results are completely outside the range that has been observed of -2 ‰ to +3 ‰. This demonstrates that further work is necessary to improve results for low concentration natural samples.

5.4 Conclusion

Pure molybdenum reference materials are necessary to set a reference point that can be used for comparison within the lab and between different laboratories. However, there has not

been an accurate determination of the isotopic composition of a standard reference material available for all laboratories to use. Using the double-spike technique, the absolute isotopic composition of the PlasmaCal standard was determined. The technique was then applied to determine the $\delta^{98/95}$Mo values for SRM-3134 and the Curtin molybdenum rod, +0.37 ‰ and -0.32 ‰ respectively. Finally, four natural USGS reference materials were analyzed after separation using ion exchange. The low concentration samples BCR-1 and SCO-1 require further analysis due to separation difficulties. The higher concentration samples BCR-2 and SDO-1 had $\delta^{98/95}$Mo values of +0.28 ‰ and +1.5 ‰ respectively.

Chapter 6

Discussion of challenges encountered during the calibration and measurement process

6.1 Introduction

This chapter is dedicated to discussing the various challenges that were encountered throughout the thesis project, and the experiments that were performed in order to solve the problems. These are described separately so as to not interrupt the flow of the preceding chapters. I will begin by discussing the problem of electro-static charge build up on the Teflon containers used during double-spike preparation. I will then discuss a set of tests performed to find a solution to the static charge problem. Finally, I will discuss drift in the $^{92}Mo/^{95}Mo$ isotope abundance ratio of the PlasmaCal molybdenum standard that was discovered when compiling all of the data.

6.2 Static during mass measurements

A requirement for the double-spike calibration is to have high precision mass measurements for all of the isotope spikes and acids used in the double-spike preparation. These measurements were all performed using a Mettler-Toledo AT201 milligram balance. The balance has a resolution of 0.01 mg and had been calibrated on 27 Jan 2011 to ensure accuracy. As mentioned in Chapter 3, the mass measurements performed on PFA bottles had uncertainties much larger than the desired uncertainty of <0.1 mg. The details of these measurements and their implications follow.

For all mass measurements the mass was measured 5 to 10 times consecutively to determine the uncertainties. First, a set of measurements of the empty bottle was performed, then

a set of measurements for the bottle with the first substance added (e.g. ORNL ^{92}Mo spike), and then a set of measurements with the second substance added (e.g. 3% HNO_3). All measurements were performed with the bottle lid securely attached. The mass of each substance was calculated by taking the difference of each measurement. This minimized systematic error in the measurement. Table 6.1 shows an example of this process from the preparation of the double-spike ABI-2. The uncertainty is expected to be close to 0.01 mg, however it is more than 100x greater than this. The double-spike calibration is highly sensitive to uncertainties in the measurements of the mass of the bottles and solutions, so measurement uncertainties must be much less than 1 mg in order to ensure that the uncertainty in the mass measurement does not dominate the propagated uncertainty.

#	Mass - Bottle (g)	Mass - With PSA (g)	Mass - With PSB (g)
1	67.94012	80.60263	86.93300
2	67.93657	80.60293	86.93204
3	67.93204	80.60238	86.93203
4	67.93798	80.60241	86.92948
5	67.93490	80.59455	86.93056
6	67.93018		
7	67.93642		
8	67.92813		
9	67.92500		
10	67.93824		
Average	67.9339	80.6010	86.9314
σ (1 s.d.)	0.0049	0.0036	0.0014

Table 6.1: Measured masses for preparation of ABI2 double-spike. The uncertainty is more than 100x greater than expected due to changing static conditions on the Teflon bottle.

The cause of this uncertainty was determined to be an electrostatic charge build-up on the bottles, which were made from perfluoroalkoxy (PFA or Teflon). Although all measurements were performed in a clean room while wearing nitrile gloves, any time a bottle was handled the measured mass could change by as much as several milligrams. This led to relatively high uncertainties during all mass measurements of samples in these bottles.

The precisions of the mass measurements of the primary and double-spikes were not op-

timal, but they were sufficient for this project as we were able to obtain <1.5 ‰ relative uncertainty for the calibrated isotope ratios of the PlasmaCal reference material. The uncertainty does make up a large portion of the uncertainty for the double-spike calibration, though the propagated uncertainty is sufficient to yield third decimal place precision for the atomic weight calculation. Also, the cost of replacing the spike material was too high for this project. However, for future preparations of mixtures, the uncertainty must be improved.

A possible solution to the problem of static charge build-up is to change the material of container used for preparation of the spikes. Although we were required to use the mixtures already prepared in Teflon bottles due to the cost of replacing them, some experiments were performed to test other possible containers and are described below.

6.3 Suitability of glass flasks for preparation of double-spikes

Borosilicate glass flasks were tested to determine their suitability for weighing out spike materials. The mass of a glass flask was first measured empty, then with a small amount of 3 % HNO_3, and then with the flask full of 3 % HNO_3. Each measurement was repeated ten times to determine the uncertainty. The measurements of the partially full then completely full flasks were done to replicate the conditions of preparing the spike mixtures. Table 6.2 demonstrates the substantial increase in precision by using glass instead of PFA. The higher uncertainty in the full bottle measurement was most likely due to some evaporation of the acid especially over the first five measurements, which caused the measured mass of solution to decrease. All measurements have much improved precision, less than 0.1 mg for the first two. This is a very positive result demonstrating that borosilicate glass is an excellent container for mixing and performing high precision mass measurements.

There is a second requirement if a container is to be used for these measurements. The container must not contaminate the sample with any elements being measured, or other compounds that could cause interferences. The glass flask with the added acid was left

Run #	Mass - Bottle (g)	Mass - 0.5 mL HNO_3 (g)	Mass - Full Bottle (g)
1	44.67466	45.19343	92.06469
2	44.67480	45.19351	92.06427
3	44.67472	45.19347	92.06408
4	44.67479	45.19348	92.06382
5	44.67477	45.19355	92.06368
6	44.67478	45.19356	92.06352
7	44.67488	45.19358	92.06336
8	44.67487	45.19360	92.06337
9	44.67486	45.19363	92.06324
10	44.67480	45.19365	92.06321
Average	44.67479	45.19355	92.06372
σ (1 s.d.)	0.00007	0.00007	0.00049

Table 6.2: Measured masses for the borosilicate glass flask. The uncertainty is substantially improved over PFA, closer to the limit of the balance.

sealed overnight in the clean room. The following day, the molybdenum and zirconium content of the acid was measured on the mass spectrometer using the secondary electron multiplier to test for interferences at the molybdenum mass range. The amounts of zirconium and molybdenum were compared against those in fresh 3 % HNO_3 to look for any sizeable increase. In Figure 6.1, we see that the signal intensity for molybdenum, zirconium, and ^{93}Nb increased substantially for the acid recovered from the glass flasks compared to the fresh acid. This demonstrates a substantial increase in the amount of zirconium, molybdenum and other substances in the acid after overnight storage. This would contaminate any samples prepared in these glass flasks. To ensure there was no residue inside the containers, they were cleaned in a nitric acid bath for one week, and the experiment was repeated with similar results showing ongoing contamination. Therefore, borosilicate glass cannot be used for any experiments involving molybdenum or zirconium.

6.3.1 Suitability of polypropylene centrifuge tubes for preparation of double-spikes

Almost all of the samples measured in the laboratory are stored in 15 mL and 50 mL polypropylene centrifuge tubes for analysis. These are the containers that are taken directly to the mass spectrometer where the liquid is sampled and analyzed. They have therefore

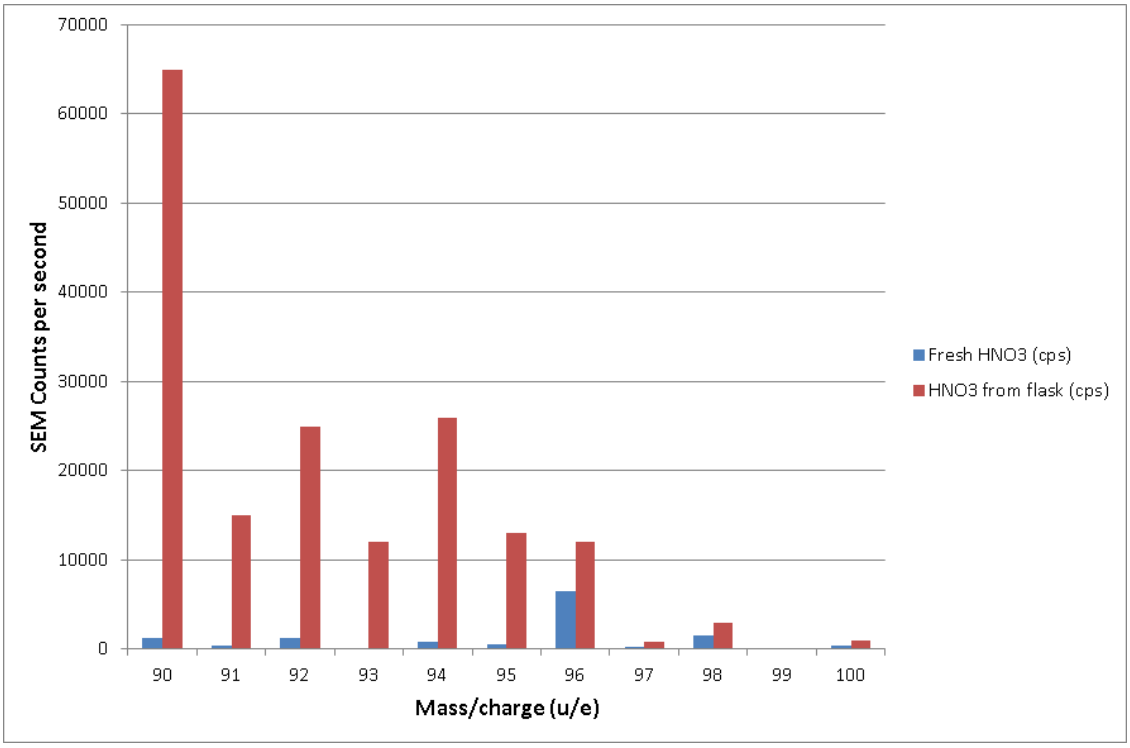

Figure 6.1: Comparison of the measured background in counts per second (cps) over the range of masses around molybdenum. There is a substantial increase in all background intensities after the acid has been left in a borosilicate flask overnight.

already been tested and shown to be free from interferences. For example, this was shown above for the fresh 3 % HNO_3 that was used as the baseline for molybdenum and zirconium content. They are therefore suitable for the initial preparation and high precision mass measurements. A centrifuge tube was tested by repeatedly measuring the mass both empty and with some liquid. In Table 6.3, we see a marked improvement over the PFA container, similar to the precision of the the glass container. These centrifuge tubes would therefore be highly suitable to the task of preparing spike materials in the future.

Run #	Mass - PPE Bottle (g)	Mass - With H_2O (g)
1	14.85569	25.93392
2	14.85565	25.93378
3	14.85570	25.93363
4	14.85571	25.93415
5	14.85581	25.93411
6	14.85569	25.93399
7	14.85574	25.93390
8	14.85578	25.93405
9	14.85576	25.93413
10	14.85582	25.93417
Average	14.85574	25.93398
σ (1 s.d.)	0.00006	0.00018

Table 6.3: Measured masses for the polypropylene centrifuge tube. The uncertainty is similar to that of borosilicate glass, while the container is free from contamination.

6.4 Standard-sample bracketing linearity test

The drift in instrumental mass bias was monitored using standard-sample bracketing, as outlined in Section 3.6. The main assumption applied to standard-sample bracketing is that the mass bias changes linearly over a period of time of approximately two hours. This assumption was tested by examining the results of seven consecutive measurements of the PlasmaCal molybdenum reference material as shown in Section 4.5. The average relative fractionations of each run as compared to the first run are shown in Table 6.4. The predicted relative fractionation differs from the measured relative fractionation by no more than 0.08

‰/amu. This source of uncertainty was incorporated into all uncertainty propagations where standard-sample bracketing was applied.

Run Time (hh:mm)	Measured α	Predicted α	Difference (‰/amu)
14:11	0	-	-
14:43	0.024	0.023	-0.009
15:17	0.048	0.040	-0.077
15:51	0.056	0.055	-0.016
16:23	0.062	0.056	-0.062
16:59	0.055	0.062	0.072
17:27	0.063	-	-

Table 6.4: Comparison of predicted and measured relative fractionations as compared to the first measurement. The predicted relative fractionation is calculated for a run using the measured fractionation of the runs before and after the run in being predicted using the equations in Section 3.6.

6.5 Long term drift of the ^{92}Mo/^{95}Mo isotope abundance ratio

All measurement sessions were started with a measurement of the PlasmaCal molybdenum reference material. This was done to ensure comparability between measurement sessions and to make sure the instrument was operating properly. Over the course of the project, I observed that there was a larger uncertainty on the ^{92}Mo/^{95}Mo isotope amount ratio as compared to the other ratios. I also observed that normalized measurements of the ^{92}Mo/^{95}Mo isotope amount ratio on the PlasmaCal standard were around 1-2 ‰ higher in February 2012 than they were in February 2011. This trend can be seen in Figure 6.2, which compares the normalized ^{92}Mo/^{95}Mo and ^{97}Mo/^{95}Mo isotope amount ratios of the first PlasmaCal run of each day over the entire measurement period. While the ^{97}Mo/^{95}Mo isotope amount ratio changes by no more than 200 ppm during the entire one year period, the ^{92}Mo/^{95}Mo isotope amount ratio changes by as much as 2000 ppm with a trend towards higher values later on. The other isotope ratios behave similarly to the ^{97}Mo/^{95}Mo isotope amount ratio.

This variability could be caused by an increase in the background at ^{92}Mo leading to an

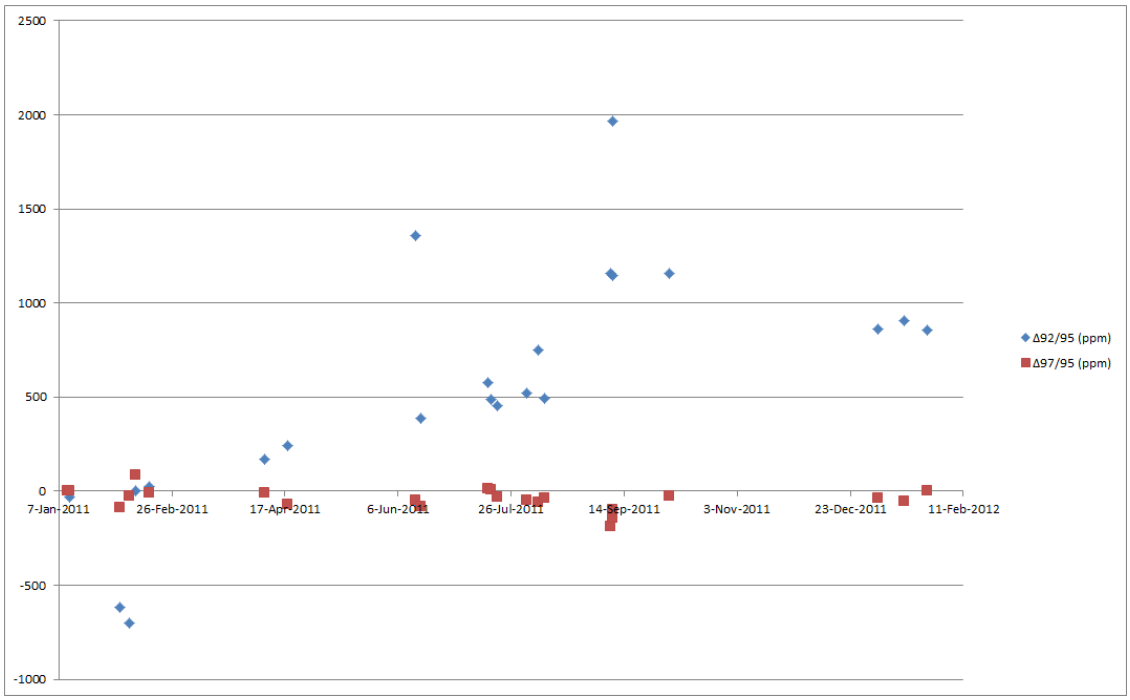

Figure 6.2: This plot compares the ppm change in the ^{92}Mo/^{95}Mo and ^{97}Mo/^{95}Mo isotope amount ratios as compared to the first value. The ^{92}Mo/^{95}Mo isotope amount ratio changes by up to 2 ‰ while the ^{97}Mo/^{95}Mo only varies by < 200 ppm.

increase in the ^{92}Mo/^{95}Mo isotope amount ratio. This is possible since ^{92}Mo is one of the spiked isotopes and can also have an interference from ^{92}Zr. A method of testing this is to measure a series of PlasmaCal standards with increasing molybdenum concentration. As the molybdenum concentration increases, the intensity of the ^{92}Mo signal from the sample increases compared to the background signal which remains constant. This would cause the anomaly on the ^{92}Mo/^{95}Mo isotope amount ratio to decrease with increasing molybdenum concentration. ^{96}Mo has already been observed to have a spectral interference of unknown origin, so it is used to demonstrate this affect as shown in Figure 6.3. As the concentration increases from 100 ppb to 2000 ppb, the ratio decreases towards its correct value. However, in Figure 6.4 we do not see the same trend. This means that there is minimal background interference at ^{92}Mo.

It is most likely that the problem was caused by a malfunctioning Faraday cup used to measure ^{92}Mo. The magnitude of the variability will substantially affect all of the data in

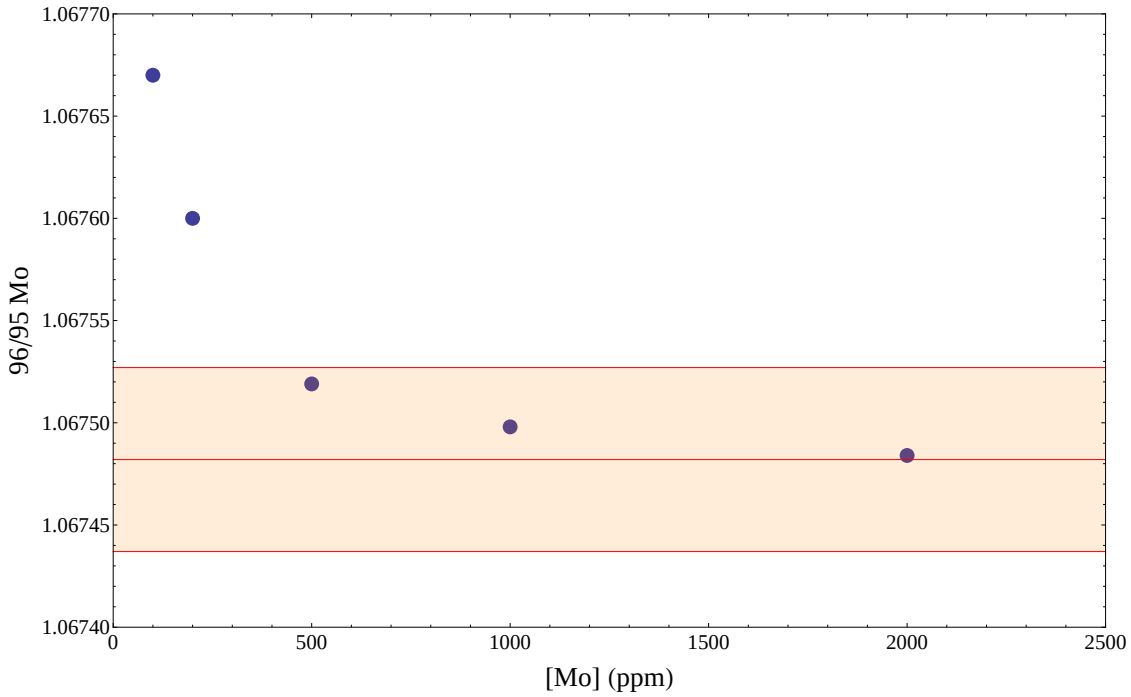

Figure 6.3: This plot shows the change in the ^{96}Mo/^{95}Mo isotope amount ratio as the concentration is increased. This is caused by the measurable interference at ^{96}Mo. Also shown is the uncertainty range based on measurements throughout the project of ∼50 ppm.

this project and cannot be corrected for with any certainty. Replacing the Faraday cup and retaking the data was not possible in time for this project and was not necessary as the focus of the project is on the analysis and methodology. After the measurement period for the project, the Faraday cup was replaced. This resulted in better reproducibility in line with the other Faraday cups, and the ^{92}Mo/^{95}Mo isotope amount ratio for PlasmaCal returned to its original value.

6.6 Summary

The double-spike calibration requires high precision mass measurements for all of the materials being prepared. The mixtures and solutions were originally prepared in PFA containers, which were highly susceptible to a build-up of electro-static charge. This led to higher uncertainties in the mass measurements and higher uncertainties in the calibration of the molyb-

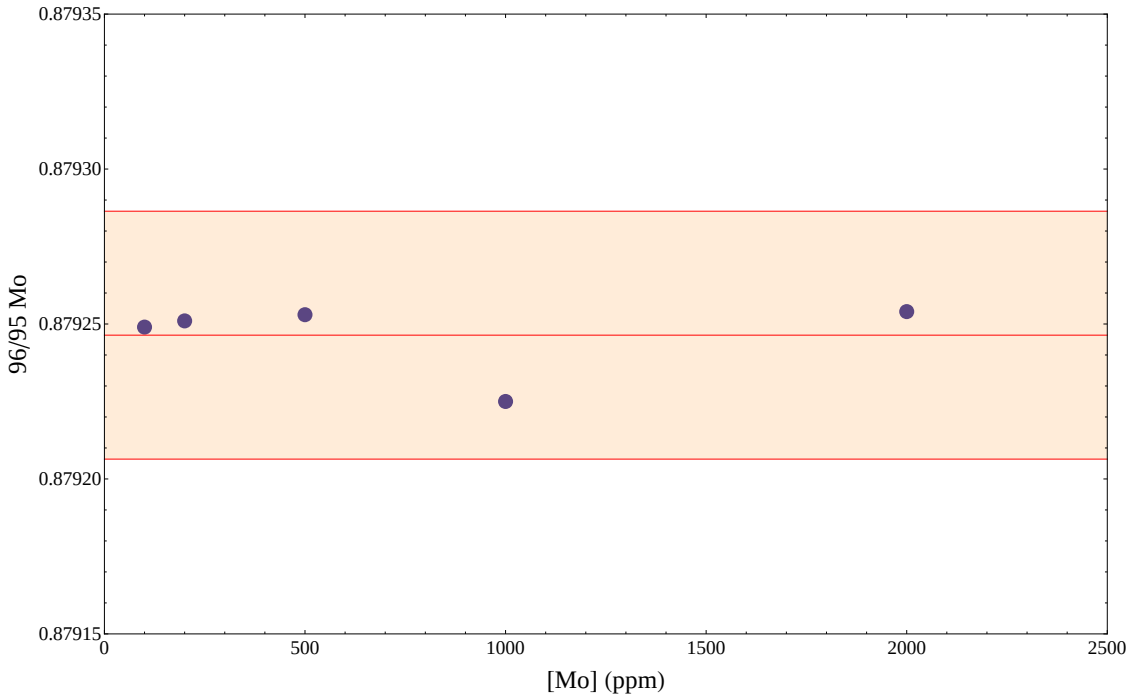

Figure 6.4: This plot shows no trend in the $^{92}Mo/^{95}Mo$ isotope amount ratio as the concentration is increased, demonstrating that there is minimal background interference at ^{92}Mo. Also shown is the uncertainty range based on measurements throughout the project of ∼50 ppm.

denum double-spikes. Borosilicate glass and polypropylene centrifuge tubes were tested as suitable replacements for all future measurements. Borosilicate glass was proven to be ineffective, as molybdenum and zirconium were constantly present in clean acids after being stored in the glass flasks. The polypropylene centrifuge tubes proved highly effective, as they were not susceptible to the electro-static buildup, there was no increase in the molybdenum and zirconium amounts in fresh acids stored in the tubes, and the mass measurements had the best possible precision. Finally, an analysis of the PlasmaCal measurements throughout the entire project showed a substantial change of up to 2000 ppm in the ^{92}Mo/^{95}Mo isotope amount ratio, while the other ratios remained relatively constant, within 200 ppm. After the measurements for this project were completed, the Faraday cup that was measuring ^{92}Mo was replaced. This proved successful as the ^{92}Mo/^{95}Mo isotope amount ratio for PlasmaCal returned to its initial value, and the stability on that Faraday cup improved to the expected level for all of the Faraday cups.

Chapter 7

Summary and conclusions

Measuring the isotopic composition of molybdenum has become an important tool in many different applications in such fields as geology[23], astronomy[25] and nuclear physics[26]. The large number of diverse applications has many different research groups publishing new and exciting results regularly. However, it has been difficult to compare the results from different laboratories since they compare their results to different reference materials. No internationally available reference material has been fully calibrated for isotopic composition. It is therefore necessary to establish the molybdenum isotopic composition of a standard reference material that can be used by all laboratories, allowing for the inter-comparison of isotope data.

I have developed a technique for determining the absolute isotopic composition of molybdenum reference materials using fully calibrated molybdenum isotope double-spikes. The calibration was done by preparing highly accurate gravimetric mixtures of ORNL ^{92}Mo and ^{98}Mo isotope spikes, and measuring the isotopic composition of the mixtures. The mass bias was corrected by using a combination of standard-sample bracketing and the calculations described in Chapter 3. The instrumental fractionation exponent was determined to be 1.444(28), which was used to calibrate the isotopic composition of the double-spike ABI-2, as shown in Table 7.1.

Sample	92/95	94/95	96/95	97/95	98/95	100/95
ABI2	146.90(14)	1.1560(4)	0.8572(5)	0.7821(5)	93.44(8)	0.7285(10)

Table 7.1: Absolute isotope ratios for double-spike ABI2.

The double-spike was mixed with a selection of synthetic reference materials, which had only been calibrated for concentration. The SCP Science - PlasmaCAL standard was chosen as our internal laboratory standard, and the absolute isotopic composition was determined

using the algorithm described in Chapter 3. The isotopic composition and atomic weight of PlasmaCAL, along with the most recent determination of the isotopic composition of molybdenum are shown in Table 7.2.

Isotope	Isotope abundance ratio ($/^{95}$Mo)	Isotopic Composition (%)	Previous best measured composition	Representative composition (IUPAC)
92	0.9217(8)	14.626(17)	14.525(15)	14.53(30)
94	0.57862(17)	9.182(5)	9.151(7)	9.15(9)
95	1(0)	15.869(5)	15.837(10)	15.84(11)
96	1.0506(4)	16.67(3)	16.672(19)	16.67(15)
97	0.6040(4)	9.585(3)	9.599(7)	9.60(14)
98	1.5318(13)	24.308(14)	24.391(18)	24.39(37)
100	0.6149(9)	9.758(11)	9.82(5)	9.82(31)
Atomic weight: 95.9508(16)			95.9602(23)	95.96(2)

Table 7.2: The isotope ratios, absolute isotopic composition and atomic weight of Plasma Cal molybdenum reference material. The previous measured isotopic composition by Wieser and De Laeter[1], and IUPAC representative composition are also reported[2].

The uncertainty of the atomic weight of molybdenum has been substantially improved from the current published value from IUPAC. The value is also more similar to the values published for the atomic weight since 1938. Due to some difficulties outlined in Chapter 6, most importantly the drift in the $^{92/95}$Mo ratio, the value is not yet ready to be submitted to IUPAC. However, the algorithm for determining the absolute isotopic composition has been established, and the Neptune mass spectrometer has been repaired. It will be possible to take an improved set of measurements in order to ensure the accuracy of the data, which will then be submitted to IUPAC for consideration in the Periodic Table of the Elements.

The natural variation of the isotopic composition of molybdenum has a $\delta^{98/95}$Mo of -1.5‰ to +3‰[7]. Applying this range to the atomic weight calculation gives the range in the atomic weight of molybdenum in natural samples of is 95.948 to 95.956. This range is larger than the uncertainty of the atomic weight of PlasmaCAL but is less than the uncertainty of the published IUPAC value. I therefore submit that the atomic weight of molybdenum in natural samples is A_r = [95.948, 95.956].

Appendix A

Mathematica code: DS-Calibration.nb

Mathematica file "DS-Calibration.nb", used to calibrate for double-spike calibration.

In[1]:=
```
masr[i_, j_] := masslist[[i]] / masslist[[j]]; (*for exp*)
masd[i_, j_] := masslist[[i]] - masslist[[j]]; (*for linear*)
Frac[v_, i_, j_, A_] := If[A == 1, masr[i, j]^v, (1 + v * masd[i, j])];
(*A=1 for exponential, A≠1 for linear*)

m0[k_] := Table[(λ[k]) * psa0[[i]] + (1 - λ[k]) * psb0[[i]], {i, 1, 7}];
psa0 := Table[psa[[i]] / Frac[α, i, ref, flaw], {i, 1, 7}];
psb0 := Table[psb[[i]] / Frac[α, i, ref, flaw], {i, 1, 7}];

λ[k_] := (1 + (mPsb[[k]] / mPsa[[k]]) *
       (Sum[psa0[[i]] * masslist[[i]], {i, 7}] / Sum[psb0[[i]] * masslist[[i]], {i, 7}]))^
    (-1); (*Derived from formula in Double Spike toolbox paper*)


Eq[i_] := m0[i][[dsI]] == AB[[i]] / Frac[α, dsI, ref, flaw]
(*This is the equation to be solved*)
```

In[9]:=
```
flaw = 1; (* 1 for Exponential, 2 for Linear*)
ref1 = 3; (*Reference Isotope (denominator) of original ratios*)
ref = 1;  (*Reference Isotope of Double Spike ratio*)
dsI = 6; (*Double Spike ratio (numerator) *)

psa := psa1 / psa1[[ref]]; (*Changing reference isotope to that of the double spike *)
psb := psb1 / psb1[[ref]];

RR7 := Table[RandomReal[NormalDistribution[]], {7}] (*Random Tables for Error Calc*)
RR10 := Table[RandomReal[NormalDistribution[]], {10}]
RR1 := RandomReal[NormalDistribution[]]

masslist =
  {91.906811, 93.9050883, 94.9058421, 95.9046795, 96.9060215, 97.9054082, 99.907477};

(*Error's are in lists where 1st element is the error table,
and 2nd element is zero error*)
Spsa1 :=
  {172.408961, 1.293911, 1., 0.691418, 0.345321, 0.847450, 0.601226} * PsaError[[PSE]];
Spsb1 := {0.576574, 0.459239, 1., 1.644201, 2.817413, 520.595025, 1.588817} *
   PsbError[[PSE]];

SAb[1] := {1.324681, 0.696948, 0.346909, 0.188002, 0.097261, 0.860604799,
    1.256259722, 2.771030135, 5.469388631, 11.74070792} * ABError[[ABE]];


SconcA := 1.2075 + cAError[[ConcE]];
SconcB := 1.6080 + cBError[[ConcE]];

Smpsa[1] := ({13.01774, 12.66702, 12.55592, 12.46411, 15.32065, 9.72988,
      6.70376, 2.99922, 1.51208, 0.71027} + MA1Error[[MassE]]) * concA;
Smpsb[1] := ({12.41546, 6.330442, 3.100458, 1.645872, 1.036306, 6.02080,
      6.05544, 6.01098, 6.01494, 6.07866} + MB1Error[[MassE]]) * concB;
```

```
PsaError := {1 + RR7 / 10^6 * {151.16, 11.93, 0, 10.50, 12.37, 284.29, 25.02}, 1};
PsbError := {1 + RR7 / 10^6 * {40.08, 23.07, 0, 19.04, 28.82, 72.64, 54.17}, 1};
ABError := {1 + RR10 * 1000 / 10^6, 1};
cAError := {RR1 * 0.0004, 0};
cBError := {RR1 * 0.0008, 0};
MA1Error := {RR10 * {0.004659309, 0.006102233, 0.008963524,
     0.010406427, 0.004718756, 0.00055, 0.00053, 0.00089, 0.00051, 0.00085}, 0};
MB1Error := {RR10 * {0.002530032, 0.003861052, 0.000788835, 0.000543001,
     0.002255926, 0.00084, 0.000470, 0.00107, 0.00060, 0.00091}, 0};


(*Error Switch; 1 for on, 2 for off*)
MassE = 1;
ConcE = 1;
PSE = 1;
ABE = 1;

DSset = 1;
AB := Ab[DSset];
mPsa := mpsa[DSset];
mPsb := mpsb[DSset];
```

In[41]:=
```
InitRand := Module[{},   (*This Initializes the random values for each value*)
   psa1 = Spsa1;
   psb1 = Spsb1;
   Ab[1] = SAb[1];
   concA = SconcA;
   concB = SconcB;
   mpsa[1] = Smpsa[1];
   mpsb[1] = Smpsb[1];
  ];
```

In[42]:=
```
it = 1000;      (*Number of iterations*)
abList = {1, 2, 3, 4, 6, 7, 8, 9, 5, 10}; (*Defines which mixtures to use*)
nn = Length[abList];
counter = 0;
Dynamic[counter]
For[k = 1, k ≤ nn, k++,
  list[k] = {};];    (*Clears all lists,
which will contain the list of alphas calculated for each Mixture*)


For[i = 1, i <= it, i++,
  InitRand;
  out = Table[FindRoot[Eq[j], {α, -1.5}, AccuracyGoal → 6], {j, abList}];

  For[k = 1, k ≤ nn, k++,
   list[k] = Append[list[k], α /. out[[k]]]];
  (*Appends each alpha to each respective list*)

  If[Mod[i, 5] == 0, counter = i];  (*Counter to see how calculation is running*)

 ];

listMean = Table[Mean[list[k]], {k, 1, nn}]
(*List of the mean alphas for each mixture*)
listSD = Table[StandardDeviation[list[k]], {k, 1, nn}]
(*List of the StDev of alphas for each mixture*)
```

Out[46]= 1000

Out[49]= {1.45101, 1.45062, 1.44791, 1.46184, 1.43279, 1.46794, 1.43437, 1.40733, 1.21171, 1.49259}

Out[50]= {0.0204258, 0.0232606, 0.0219514, 0.0242228,
 0.018997, 0.0185591, 0.0200091, 0.0192807, 0.0404908, 0.0265472}

In[51]:=
```
TableForm[{listMean, listSD}]
```

Out[51]//TableForm=

1.45101	1.45062	1.44791	1.46184	1.43279	1.46794	1.43437
0.0204258	0.0232606	0.0219514	0.0242228	0.018997	0.0185591	0.0200091

In[52]:=
```
FullList = Union[list[1], list[2], list[3], list[4], list[5], list[6], list[7], list[8]];
Mean[FullList]
StandardDeviation[FullList]
```

Out[53]= 1.44423

Out[54]= 0.0275312

Appendix B

Mathematica code: Double-spike uncertainty.nb

Mathematica file "Double-spike uncertainty.nb", used to propagate uncertainty in double-spike isotopic composition and PlasmaCAL standard isotopic composition and atomic weight.

In[1]:=
```
masslist={91.906811,93.9050883,94.9058421,95.9046795,96.9060215,97.9054082,
 99.907477};
flaw=1;
ref=3;
masr[i_,j_]:=masslist[[i]]/masslist[[j]]; (*for exp*)
masd[i_,j_]:=masslist[[i]]-masslist[[j]]; (*for linear*)
Frac[v_,i_,j_,A_]:=If[A==1,masr[i,j]^v,(1+v*masd[i,j])];
RR1:=RandomReal[NormalDistribution[]]
RR7:=Table[RandomReal[NormalDistribution[]],{7}]
RatF[ratios_,α_]:=Table[ratios[[j]]*Frac[α,j,ref,flaw],{j,7}]
AtWgt[ratios_]:=Total[masslist*ratios/(Total[ratios])]
FracTable[α_]:=Table[Frac[α,i,ref,flaw],{i,7}]

αcalc[sta_,spi_,mix_]:=Module[{s,s0,m,m0,t0,pSpike,AwP,AwS,mp,ms,mapercS,mapercP,out}
    m0:=Table[(1-λ)*s0[[i]]+(λ)*t0[[i]],{i,1,7}];
    s0:=Table[s[[i]]/Frac[α,i,ref,flaw],{i,1,7}];
    Eq[i_]:=m[[i]]/Frac[β,i,ref,flaw]-m0[[i]]==0;
    Eqtable:=Table[Eq[ratList[[i]]],{i,1,3}];
    ratList={1,6,5};

    s=sta;
    m=mix;
    t0=spi;
    out=FindRoot[Eqtable,{{α,.1},{β,.1},{λ,.1}}];

    (*Mass % Calculation*)
    pSpike:=(1+(1-λ)/λ*(Sum[s0[[i]],{i,1,7}]/Sum[t0[[i]],{i,1,7}]))^(-1);
    AwP:=Sum[t0[[i]]*masslist[[i]],{i,7}]/Sum[t0[[i]],{i,7}];
    AwS:=Sum[s0[[i]]*masslist[[i]],{i,7}]/Sum[s0[[i]],{i,7}];
    mp:=pSpike*AwP;
    ms:=(1-pSpike)*AwS;
    mapercS:=ms/(ms+mp);
    mapercP:=mp/(ms+mp);

    out1={MpP->mapercP*100/.out,out[[1]]};
    Return[out1];
];
```

In[13]:=
```
ABI2 = {140.24, 1.13842, 1., 0.8703, 0.806056, 97.739, 0.7846};
ABI2u = {0.04, 0.00013, 0, 0.0004, 0.000009, 0.020, 0.0004};
α1 = 1.444;
α1u = 0.028;

(*Standard α and uncertainty from Absolute Standard uncertainty*)
std := {0.880210, 0.569898, 1., 1.066458, 0.622335, 1.601633, 0.661899};
stdu := {0.000012, 0.000004, 0, 0.000206, 0.000006, 0.000016, 0.000012};
(*uncertainty in 96/95 expanded due to known interference of unknown origin*)
αS = 1.433;
αSu = 0.028;
```

In[21]:=
```
it = 10 000;
ABlist = {};
For[i = 1, i ≤ it, i++,
  ABI2e = ABI2 + RR7 * ABI2u;
  αe = α1 + RR1 * α1u;
  ABI2ce = ABI2e * FracTable[-αe];
  ABlist = Append[ABlist, ABI2ce];
 ];
MeanAB = Mean[ABlist];
SDAB = StandardDeviation[ABlist];
TableForm[{MeanAB, SDAB}]
```

[26]//TableForm=

146.895	1.15598	1.	0.857237	0.782142	93.4444	0.728516
0.138475	0.000365436	0.	0.000470303	0.000455011	0.0830809	0.00110876

In[45]:=
```
it = 10 000;
stdlist = {};
AWlist = {};
IClist = {};
For[i = 1, i ≤ it, i++,
  stde = std + RR7 * stdu;
  αSe = αS + RR1 * αSu;
  stdce = stde * FracTable[-αSe];
  stdlist = Append[stdlist, stdce];
  IClist = Append[IClist, stdce / Total[stdce]];
  AWlist = Append[AWlist, AtWgt[stdce]];
 ];
Meanstd = Mean[stdlist];
SDstd = StandardDeviation[stdlist];
TableForm[{Meanstd, SDstd}]
MeanIC = Mean[IClist];
SDIC = StandardDeviation[IClist];
Print[];
TableForm[{MeanIC * 100, SDIC * 100}]
Mean[AWlist]
StandardDeviation[AWlist]
```

[52]//TableForm=

0.921664	0.578622	1.	1.05057	0.604008	1.53178	0.614929
0.000830804	0.000172123	0.	0.000366453	0.000353511	0.00133799	0.000886

[56]//TableForm=

14.6259	9.18219	15.8691	16.6716	9.58504	24.3078	9.7583	
0.0175524	0.00547795	0.00476137	0.00270091	0.00276912	0.0140045	0.0111	

Out[57]= 95.9508

Out[58]= 0.00161198

In[59]:=
```
(*Natural Range*)
D98Hi = 3;
D98Lo = -1.5;
DAConv[δ_] := Log[δ / 1000 + 1] / Log[masslist[[6]] / masslist[[3]]]
AtWgt[std * FracTable[-αS + DAConv[D98Hi]]]
AtWgt[std * FracTable[-αS + DAConv[D98Lo]]]
```

Out[62]= 95.9563

Out[63]= 95.948

Appendix C

Mathetmatica Code - Absolute standard uncertainty.nb

Mathematica file "Absolute Standard Uncertainty.nb", used to determine uncertainty in PlasmaCAL fractionation exponent.

```
(*Requires Double-spike uncertainty.nb*)
```

In[2]:=
```
Openfiles := Module[{files, tempratio, i, importlistS},
   (*outputs variables importratioS and filenames*)
   files = SystemDialogInput["FileOpen", {"", {"Data export" → {"*.exp"}}}];
   If[files == $Canceled, Return[]];
filenames =
    Table[StringTake[files[[i]], {Last[StringPosition[files[[i]], "\\"]][[1]] + 1,
       StringLength[files[[i]]]}], {i, Length[files]}];
   importlistS = Table[Import[files[[i]]], {i, Length[files]}];
   importratioS =
    Table[{filenames[[j]], Insert[Table[importlistS[[j]][[4]][[i]], {i, 4, 4 + 5}], 1, 3]
     {j, Length[files]}];
Return[importratioS];
];
```

In[3]:=
```
Openfiles
```

Out[3]=
```
{{009 - DSM45.exp, {3.65015, 0.578314, 1, 1.06847, 0.632612, 3.6073, 0.682091}},
 {010 - DSM50.exp, {4.22343, 0.580683, 1, 1.0676, 0.633286, 4.0136, 0.682384}},
 {011 - DSM55.exp, {4.98179, 0.583856, 1, 1.06652, 0.634273, 4.5521, 0.682871}},
 {012 - DSM45.exp, {3.65421, 0.578512, 1, 1.06791, 0.63217, 3.60359, 0.680776}},
 {012 - DSM60.exp, {5.88104, 0.587578, 1, 1.06514, 0.635389, 5.19027, 0.683515}},
 {014 - DSM50.exp, {4.22842, 0.580952, 1, 1.06702, 0.632828, 4.00941, 0.680927}},
 {016 - DSM55.exp, {4.98706, 0.584098, 1, 1.06589, 0.633821, 4.547, 0.681394}},
 {018 - DSM43.exp, {3.42357, 0.577595, 1, 1.06828, 0.631769, 3.4384, 0.680335}},
 {018 - DSM60.exp, {5.88759, 0.587824, 1, 1.06453, 0.634945, 5.1846, 0.682137}},
 {026 - DSM43.exp, {3.42642, 0.57778, 1, 1.06786, 0.631438, 3.43566, 0.679252}},
 {041 - DSM55.exp, {4.98947, 0.584185, 1, 1.06578, 0.633623, 4.5452, 0.681017}},
 {042 - DSM60.exp, {5.88804, 0.587854, 1, 1.06474, 0.634935, 5.18439, 0.682107}},
 {046 - DSM43.exp, {3.42438, 0.577636, 1, 1.06817, 0.631666, 3.43774, 0.680065}}}
```

In[42]:=
```
(*Uncertainty in α-correction for ABI-2 not propagated*)

ratList = {1, 6, 5};
Nfiles = Length[importratioS];
ABI2c = ABI2 * FracTable[-1.444];
oTable = {};
For[i = 1, i ≤ Nfiles, i++,
  out = αcalc[std, ABI2c, importratioS[[i]][[2]]];
  oTable = Append[oTable, {MpP /. out, α /. out, filenames[[i]]}];
 ];
oTable = Sort[oTable];
oTable = Prepend[oTable, {"Mass % Spike", "α calc", "FileName"}];
oTable // TableForm
```

[49]//TableForm=

Mass % Spike	α calc	FileName
41.9884	1.42893	026 - DSM43.exp
41.9885	1.42993	018 - DSM43.exp
41.9901	1.43187	046 - DSM43.exp
44.1566	1.43217	009 - DSM45.exp
44.1575	1.43186	012 - DSM45.exp
48.9111	1.43303	010 - DSM50.exp
48.9128	1.43266	014 - DSM50.exp
54.1302	1.4318	016 - DSM55.exp
54.1321	1.43363	041 - DSM55.exp
54.1321	1.43258	011 - DSM55.exp
59.1446	1.43531	018 - DSM60.exp
59.1447	1.43388	042 - DSM60.exp
59.1455	1.43723	012 - DSM60.exp

In[50]:=
```
αlist = Table[oTable[[i]][[2]], {i, 2, Nfiles + 1}];
Mean[αlist]
StandardDeviation[αlist]
```

Out[51]= 1.43268

Out[52]= 0.00212242

In[59]:=
```
(*Uncertainty in α-correction for ABI-2 propagated*)

it = 500;
αelist =.;
For[k = 1, k ≤ Nfiles, k++,
  αelist[k] = {};
  mixi = importratioS[[k]][[2]];
  For[i = 1, i ≤ it, i++,
   ABI2ce = ABI2 * FracTable[-(α1 + RR1 * α1u)];
   αelist[k] = Append[αelist[k], α /. αcalc[std, ABI2ce, mixi][[2]]]
  ];
  importratioS[[k]][[1]];
  m1 = Mean[αelist[k]];
  sd1 = StandardDeviation[αelist[k]];
  Print[importratioS[[k]][[1]], ":  ", m1, "    ", sd1];
 ];
αelistT = Flatten[Table[αelist[j], {j, 1, Nfiles}]];
Print[];
Print["α average = ", Mean[αelistT], " ± ", StandardDeviation[αelistT]];
```

```
009 - DSM45.exp:  1.43119    0.0285655
010 - DSM50.exp:  1.43211    0.0263625
011 - DSM55.exp:  1.43376    0.0282631
012 - DSM45.exp:  1.43431    0.0272063
012 - DSM60.exp:  1.43796    0.0276641
014 - DSM50.exp:  1.43353    0.0279895
016 - DSM55.exp:  1.43262    0.0277785
018 - DSM43.exp:  1.4296    0.0283104
018 - DSM60.exp:  1.43512    0.0273156
026 - DSM43.exp:  1.42514    0.0288027
041 - DSM55.exp:  1.43246    0.0294968
042 - DSM60.exp:  1.43376    0.0286668
046 - DSM43.exp:  1.42953    0.0269825


α average = 1.43239 ± 0.0281014
```

Appendix D

Goldschmidt 2011 - Abstract

We presented our research at the 2011 Goldschmidt conference in Prague. This conference was attended by over 3000 people, and the research was well received by the community. Some of the most important people researching the molybdenum isotope system in nature including C. Siebert and J. Barling gave positive feedback on the poster presentation. Following is the printed abstract, published in Minerological Magazine.[39]

Absolute isotopic composition of molybdenum reference materials using double spike MC-ICP-MS

A.J. MAYER[1]*, B. PROEMSE[2] AND M.E. WIESER[1]

[1]Department of Physics and Astronomy, 2500 University Drive NW, University of Calgary, Calgary, AB, T2N 1N4, Canada (*correspondence: ajmayer@ucalgary.ca)
[2]Department of Geoscience, 2500 University Drive NW, University of Calgary, Calgary, AB T2N 1N4, Canada

Molybdenum isotope abundance measurements have enabled unique insights into the study of oxic conditions in the oceans [1], high-temperature hydrothermal ore deposits [2], and the heterogeneity of molybdenum in the early solar system [3]. Useful interpretations are only possible when isotopic compositions are reported relative to commonly available reference materials. Chemical processing of samples can alter isotopic composition, so it is important to test methods on matrices of known molybdenum isotopic composition and concentration.

At present, researchers are using a variety of commercially available and in-house standards. Recently, Wen *et al*. measured the relative isotopic composition of five reference solutions and proposed using NIST SRM 3134 as the delta zero reference for molybdenum [4]. However, the absolute isotopic compositions of these standards were not reported and none of the chosen materials were in a natural matrix.

In this study, we have determined the absolute isotopic composition of molybdenum in a variety of reference materials including NIST SRM 3134, BCR-1, BCR-2 (basalt), USGS SCo-1 (shale), SRM 1547 (peach leaves), Johnson-Matthey pure Mo metal rod, and SCP Science Mo PlasmaCal. Measurements were made using a Thermo Scientific Neptune MC-ICP-MS. Instrumental fractionation was corrected by measuring a mixture of the sample with a fully calibrated double spike. The fractionation correction assumed an exponential fractionation law and used computational root finding methods to solve for the fractionation due to chemical processing and instrumental mass bias.

[1] Barling *et al*. (2001) *EPSL* **193**, 447–457. [2] Mathur *et al*. (2010) *Miner Deposita* **45**, 43–50. [3] Dauphas *et al*. (2002) *ApJ*. **565**, 640–644. [4] Wen *et al*. (2010) *J. Anal. At. Spectrom*. **25**, 716–721.

Bibliography

[1] M. E. Wieser and J. R. De Laeter, "Absolute isotopic composition of molybdenum and the solar abundances of the p-process nuclides mo92,94", *Physical Review C - Nuclear Physics*, vol. 75, no. 5, 2007.

[2] M. Berglund and M. E. Wieser, "Isotopic compositions of the elements 2009 (iupac technical report)", *Pure and Applied Chemistry*, vol. 83, no. 2, pp. 397–410, 2011.

[3] USGS, "USGS certificate of analysis Devonian Ohio shale, SDO-1 (geochemical reference standards)", `http://crustal.usgs.gov/geochemical_reference_standards/ohioshale.html`, August 2012.

[4] USGS, "USGS certificate of analysis Cody shale, SCo-1 (geochemical reference standards)", `http://crustal.usgs.gov/geochemical_reference_standards/codyshale.html`, August 2012.

[5] USGS, "USGS certificate of analysis basalt, Columbia River, BCR-2 (geochemical reference standards)", `http://crustal.usgs.gov/geochemical_reference_standards/basaltbcr2.html`, August 2012.

[6] K. Govindaraju, "1994 compilation of working values and sample description for 383 geostandards", *Geostandards newsletter*, vol. 18, no. Special issue, pp. 1–158, 1994.

[7] A.D. Anbar, "Molybdenum stable isotopes: Observations, interpretations and directions", *Reviews in Mineralogy and Geochemistry*, vol. 55, pp. 429–454, 2004.

[8] K.M. Revesz, J.M. Landwehr, and J. Keybl, "Measurement of 13c and 18o isotopic ratios of caco3 using a thermoquest finnigan gasbench ii delta plus xl continuous flow isotope ratio mass spectrometer with application to devils hole core dh-11 calcite", *U.S. Geological Survey Open-File Report 01-257*, 2001.

[9] R. Thomas, "A beginner's guide to icp-ms part viii: Mass analyzers - time-of-flight technology", *Spectroscopy*, vol. 17, no. 1, pp. 36–41, January 2002.

[10] R. Thomas, "A beginner's guide to icp-ms part vi - the mass analyzer", *Spectroscopy*, vol. 16, no. 10, pp. 44–49, October 2001.

[11] TRIUMF, "Penning traps", `http://titan.triumf.ca/equipment/penning_trap/index.shtml`, August 2012.

[12] P Gates, "Methods of ion detection", `http://www.chm.bris.ac.uk/ms/theory/detection.html`, August 2012.

[13] Thermo Scientific, "Neptune plus multicollector icpms brochure", August 2012.

[14] R. Thomas, "A beginner's guide to icp-ms part ii: The sample-introduction system", *Spectroscopy*, vol. 16, no. 5, pp. 56–60, May 2001.

[15] R. Thomas, "A beginner's guide to icp-ms part iv: The interface region", *Spectroscopy*, vol. 16, no. 7, pp. 26–30, July 2001.

[16] M. E. Wieser and J. B. Schwieters, "The development of multiple collector mass spectrometry for isotope ratio measurements", *International Journal of Mass Spectrometry*, vol. 242, no. 23, pp. 97 – 115, 2005.

[17] J. F. Rudge, B. C. Reynolds, and B. Bourdon, "The double spike toolbox", *Chemical Geology*, vol. 265, no. 3-4, pp. 420–431, 2009.

[18] London Metal Exchange, "Industry usage of molybdenum", `http://www.lme.com/minormetals/6782.asp`, August 2012.

[19] W.O. Winer, "Molybdenum disulfide as a lubricant: A review of the fundamental knowledge", *Wear*, vol. 10, no. 6, pp. 422 – 452, 1967.

[20] P. C. Dos Santos and D. R. Dean, "A newly discovered role for iron-sulfur clusters", *Proceedings of the National Academy of Sciences*, vol. 105, no. 33, pp. 11589–11590, 2008.

[21] J. Barling, G.L Arnold, and A.D Anbar, "Natural mass-dependent variations in the isotopic composition of molybdenum", *Earth and Planetary Science Letters*, vol. 193, no. 3-4, pp. 447–457, 2001.

[22] C. Siebert, T.F. Nägler, F. von Blanckenburg, and J.D. Kramers, "Molybdenum isotope records as a potential new proxy for paleoceanography", *Earth and Planetary Science Letters*, vol. 211, no. 1-2, pp. 159–171, 2003.

[23] A.D. Czaja, C.M. Johnson, E.E. Roden, B.L. Beard, A.R. Voegelin, T.F. Nägler, N.J. Beukes, and M. Wille, "Evidence for free oxygen in the neoarchean ocean based on coupled iron-molybdenum isotope fractionation", *Geochimica et Cosmochimica Acta*, vol. 86, pp. 118–137, 2012.

[24] M.E. Wieser and J.R. De Laeter, "Evidence of the double β decay of zirconium-96 measured in 1.8x10^9 year-old zircons", *Physical Review C - Nuclear Physics*, vol. 64, no. 2, pp. 243081–243087, 2001.

[25] N. Dauphas, B. Marty, and L. Reisberg, "Molybdenum evidence for inherited planetary scale isotope heterogeneity of the protosolar nebula", *Astrophysical Journal Letters*, vol. 565, no. 1 I, pp. 640–644, 2002.

[26] M. E. Wieser, S. Barry, and J. R. De Laeter, "Fission yields of molybdenum in the oklo natural reactor", *Journal of Radioanalytical and Nuclear Chemistry*, pp. 1–6, 2012, Article in Press.

[27] M. E. Wieser and M. Berglund, "Atomic weights of the elements 2007 (iupac technical report)", *Pure and Applied Chemistry*, vol. 81, no. 11, pp. 2131–2156, 2009.

[28] Nobelprize.org, "The nobel prize in chemistry 1914", http://www.nobelprize.org/nobel_prizes/chemistry/laureates/1914/, August 2012.

[29] J.R. De Laeter, "The role of mass spectrometry in atomic weight determinations", *Mass Spectrometry Reviews*, vol. 28, no. 1, pp. 2–19, 2009.

[30] F.W. Aston, "The Isotopic Constitution and Atomic Weights of Zinc, Tin, Chromium and Molybdenum", *Royal Society of London Proceedings Series A*, vol. 130, pp. 302–310, Jan. 1931.

[31] T.W. Lyons and C.T. Reinhard, "Deoxygenation in warming oceans-looking back to the future", *Geology*, vol. 40, no. 7, pp. 671–672, 2012.

[32] N. D. Greber, C. Siebert, T. F. Nägler, and T. Pettke, "d98/95mo values and molybdenum concentration data for nist srm 610, 612 and 3134: Towards a common protocol for reporting mo data", *Geostandards and Geoanalytical Research*, pp. 1–10, 2012.

[33] H. Wen, J. Carignan, C. Cloquet, X. Zhu, and Y. Zhang, "Isotopic delta values of molybdenum standard reference and prepared solutions measured by mc-icp-ms: Proposition for delta zero and secondary references", *Journal of Analytical Atomic Spectrometry*, vol. 25, no. 5, pp. 716–721, 2010.

[34] R. Thomas, "A beginner's guide to icp-ms", *Spectroscopy*, vol. 16, no. 4, pp. 38–42, 2001.

[35] L. Yang, "Accurate and precise determination of isotopic ratios by mc-icp-ms: A review", *Mass spectrometry reviews*, vol. 28, no. 6, pp. 990–1011, 2009.

[36] W.A. Russell, D.A. Papanastassiou, and T.A. Tombrello, "Ca isotope fractionation on the earth and other solar system materials", *Geochimica et Cosmochimica Acta*, vol. 42, no. 8, pp. 1075–1090, 1978.

[37] M.H. Dodson, "A theoretical study of the use of internal standards for precise isotopic analysis by the surface ionization technique: Part i - general first-order algebraic solutions", *Journal of Scientific Instruments*, vol. 40, no. 6, pp. 289–295, 1963.

[38] R.D. Russell, "The systematics of double spiking", *Journal of geophysical research*, vol. 76, no. 20, pp. 4949–4955, 1971.

[39] A.J. Mayer, B. Proemse, and M.E. Wieser, "Absolute isotopic composition of molybdenum reference materials using double spike mc-icp-ms", *Minerological Magazine*, vol. Goldschmidt Conference Abstracts, pp. 1432, 2011.